CrossMark

ORIGINAL RESEARCH

Inelastic behavior of cold-formed braced walls under monotonic and cyclic loading

Mohsen Gerami[1] · Mohsen Lotfi[2] · Roya Nejat[3]

Abstract The ever-increasing need for housing generated the search for new and innovative building methods to increase speed and efficiency and enhance quality. One method is the use of light thin steel profiles as load-bearing elements having different solutions for interior and exterior cladding. Due to the increase in CFS construction in low-rise residential structures in the modern construction industry, there is an increased demand for performance inelastic analysis of CFS walls. In this study, the nonlinear behavior of cold-formed steel frames with various bracing arrangements including cross, chevron and k-shape straps was evaluated under cyclic and monotonic loading and using nonlinear finite element analysis methods. In total, 68 frames with different bracing arrangements and different ratios of dimensions were studied. Also, seismic parameters including resistance reduction factor, ductility and force reduction factor due to ductility were evaluated for all samples. On the other hand, the seismic response modification factor was calculated for these systems. It was concluded that the highest response modification factor would be obtained for walls with bilateral cross bracing systems with a value of 3.14. In all samples, on increasing the distance of straps from each other, shear strength increased and shear strength of the wall with bilateral bracing system was 60 % greater than that with lateral bracing system.

✉ Mohsen Lotfi
   mohsen.lotfi67@yahoo.com

[1] Faculty of Engineering, Semnan University, Semnan, Iran

[2] Faculty of Civil Engineering, Semnan University, Semnan, Iran

[3] Faculty of Civil Engineering, University of Mohaghegh Ardabili, Ardabili, Iran

Introduction

Today, the use of cold-formed steel members as structural elements has gained much popularity in the construction of residential and industrial buildings. One proper strategy for improving the seismic behavior of these structures is the use of structural coverage or braces. Braces transmit horizontal forces from floor and ceiling surfaces to the foundation. The overall lateral resistance of structures, hardness and ductility of these systems is not entirely confined to braces; however, the behavior of the wall is under the influence of different members of these structures in the lateral load transfer path such as brace joints, binding sheets, studs, tracks and joints. The National Building Code of Canada (2005) contains a philosophy of basic capacity for seismic design, in which a series of fuse elements is defined in seismic-resistant systems for waste of energy caused by earthquake. Fuse elements are expected to enter the nonlinear region. Other members of the frame are also designed for the capacity of the fuse elements to remain linear and experience minimal nonlinear failure. Usually, elements that play the role of fuse in these structures are braces. In the following, we will address some numerical and laboratory studies conducted by researchers on the behavior of cold-formed steel walls.

Miller and Pekoz (1993) conducted studies on the effect of cover plates on vertical load-carrying capacity of cold-formed steel studs. Serrette (1997) conducted both static and cyclic load tests on cold-formed steel walls. Tests included panels with different types of bracing, including

Springer

steel sheet sheathing. The sheathing or bracing was placed on only one side of the panels. The failure of steel sheathed panels resulted from rupture of the steel sheet along the line of screws at the edges. Decreasing the fastener spacing and increasing the steel sheathing thickness were effective in increasing the maximum load.

Gad et al. (1999a, b) presented a detailed investigation of the contribution of plasterboard in the seismic performance of CFS X-strap bracing walls and its relevant structural modification factor using experimental tests with shaker table and numerical studies. The authors reported a wide range of values between 4 and 29 for R factor, though they highlighted that the results were impractical and misleading and needed more number of research studies to be reliable.

Telue and Mahendran (2002) conducted experiments on cold-formed steel frames to investigate the behavior of plaster cover plates in the wall of these frames and concluded that the load-carrying capacity of the studs of wall panels would significantly increase if brace and cover plates were used. Fülöp and Dubina (2004) tested three X-braced screw-connected wall specimens (3.6 m long × 2.44 m high) under in-plane lateral loading. Of the three wall specimens, one was tested monotonically and two cyclically. The walls were constructed of a cold-formed steel frame. The screw connection configuration was selected to facilitate yielding along the length of the brace, i.e., to avoid net section fracture of the strap through the screw holes. Chord members were constructed of double stud members, such that inelastic deformations and ultimate failure of the walls would be limited to the braces. U profiles were placed in the tracks at corner locations to increase the hold-down capacity and rigidity. Local buckling of the lower track was observed during loading with damage being concentrated in corner areas. Plastic elongation of the strap did take place; however because of the unexpected failure of the corners, the results of the experiments may not necessarily reflect the true ductility of a braced wall if yielding (and failure) had been limited to the straps. Fülöp and Dubina suggested that the ideal configuration of the corners would be such that the uplift force is directly transmitted from the brace or corner stud to the anchoring bolt, without inducing bending in the bottom track. Failure to strengthen the corners can have a significant effect on the initial rigidity of the system and can be the cause of larger than expected in-plane shear deformations of the wall and premature failure of the braced frame.

Berman et al. (2005) investigated CFS frames using both X-braced and steel-plated shear walls. The main aim of their research was to provide an engineering guideline for evaluating both of these types of CFS walls considering stiffness, ductility and energy dissipation. They reported that the maximum initial stiffness was related to the X-braced frame specimen, while the maximum ductility was provided by steel plate shear wall. Interestingly, using scaled hysteretic results, they found that the energy dissipated was similar for both X-braced frames and steel plate shear walls. Kim et al. (2006) performed a shaker table test on a full-scale two-story one-bay CFS shear panel structure. Each story consisted of two identical shear walls of 2.8 m length and 3.0 m height separated from each other by 3.9 m center to center. The two chords were constructed from three C-sections forming a two-cell closed section, and columns were welded to steel anchors and bolted to the slab through the top and bottom tracks. A heavy square RC slab of 4.4×4.4 m^2 by 200 mm thickness along with additional mass was placed at the top of each floor level, which made the total mass at each floor level equal to 256 kN. As the second story frame was identical to the first story, the damage occurred mostly in the first story as expected. Connections and anchors to the base beam were designed for the maximum over-strength of straps, based on TI 809-07 (1998) code; however, no pre-tensioning was applied to the tension-only straps in spite of explicit recommendation in the code. The system was completely symmetrical and the centers of mass and stiffness were located at the same point and parallel to shear walls of the structure, to preclude torsional and out-of-plane responses. The structure was then loaded to a normalized accelerogram, which possessed spectral response acceleration equal to the design response spectrum around the fundamental period of the test specimen. The test caused significant yielding in the form of severe nonlinear behavior in the first floor straps along their entire length and yielding of studs near the anchors. The studs did not develop full flexural strength due to local buckling and this impaired their potential contribution to the story shear resistance. The studs' contribution further decreased (about 15 %) due to anchor deformation, which created a gap between the track and the slab. The results showed that during the large amplitude tests, the X-strap bracing showed very ductile, but highly pinched, hysteretic behavior. The results of this study can be considered conservative because the effect of non-structural gypsum board cladding was not considered in the test.

Al-Kharat and Rogers (2007) tested 16 sample walls with crossed straps in cold-formed steel frames in laboratory under cyclic and monotonic loading condition. In the research conducted by these researchers, certain criteria for behavior factor have been suggested. Scrutinizing the obtained results and comparing the results to other experiments performed by the authors (Moghimi and Ronagh 2009; Zeynalian and Ronagh 2010a, b) and other researchers show that the X-strap-braced system is considered as a ductile system with a satisfactory shear strength;

and as such the use of this kind of CFS structure can be preferable particularly in low to medium seismic regions.

Zeynalian and Ronagh (2011) presented a numerical study on seismic characteristics of knee-braced cold-formed steel shear walls. A total of 12 models with various ranges of knee elements' lengths were investigated. The numerical models were verified based on experimental tests. Agreement of the numerical simulations and the test results showed that finite element analysis can be used effectively to predict the ultimate capacity of knee-braced CFS shear panels. Of particular interests were the specimens' maximum lateral load capacity and deformation behavior in addition to a rational estimation of the seismic response modification factor. Preliminary conclusions presented in this paper refer to the optimum seismic characteristics of knee-braced CFS shear walls and the corresponding dimensions and configuration.

Pan and Shan (2011) focused on the experimental study of the structural strength of cold-formed steel wall frames with sheathing under monotonic shear loading. Based on the test result analysis, the ductility ratio of the specimen with one-side sheathing was greater than that of the specimen with two-side sheathing. The ultimate strength of wall frame with sheathing increased with increase in the thickness of board.

Zeynaliana et al. (2012) studied the lateral performance of K-braced cold-formed steel structures and their response modification coefficients, R factor. A total of 12 full-scale 2.4×2.4 m specimens of different configurations were tested under a standard cyclic loading regime. Of particular interest are the specimens' maximum lateral load capacity and deformation behavior as well as a rational estimation of the seismic response modification factor. They concluded that use of a K-stud bracing system is possible only in low seismic regions where the earthquake loads, and thus the required lateral resistance capacity, are not high.

Nithyadharan and Kalyanaraman (2012) presented a numerical model of the hysteretic behavior of such panels, necessary to study the system behavior under various earthquake loading. In this paper, Bouc–Wen–Baber–Noori (BWBN) model is used to capture the deteriorating behaviour, such as the strength and stiffness degradation with severe pinching, observed in the screw connections between the CFS framing members and sheathing, as well as the full wall panels under cyclic loading. The system identification technique based on Nelder and Mead's simplex algorithm is used to identify the unknown parameters of the model. The representation of the constitutive relationship, both under static and cyclic loading of the screw connections and the wall panel sub-system, is demonstrated using the BWBN model.

Zeynalian and Ronagh (2012a, b) studied the seismic performance of strap-brace cold-formed steel shear walls.

This paper presented a nonlinear finite element analyses to optimize the seismic characteristics of strap-braced cold-formed steel shear walls enhanced with brackets in the four interior corners of the wall. The numerical models presented here are verified based on experimental tests considering different structural characteristics including: material nonlinearity, geometrical imperfection, residual stresses and perforations. A comparison between the numerical simulations and the test results shows a good agreement proving that finite element analysis can be used effectively to predict the ultimate capacity of strap-braced CFS shear panels. A total of 16 models with different variants of bracket length are investigated. Of particular interest were the specimens' maximum lateral load capacity and deformation behavior in addition to a rational estimation of the seismic response modification factor. Preliminary conclusions presented in this paper refer to the optimum seismic characteristics of strap-braced CFS shear walls and the corresponding dimensions and configuration.

Fiorino et al. (2012) investigated the extensive parametric nonlinear dynamic analysis carried out on one story buildings by means of incremental dynamic analysis (IDA), using an ad hoc model of the hysteresis response of SCFS shear walls. Considering the results of this study, a design nomograph for the seismic design of single-story SCFS frame structures developed on the basis of nonlinear dynamic analysis results is presented. This aims to complete a proposal of a design methodology already presented by the author in the last years.

Dabreo et al. (2014) evaluated the behavior of shear walls made of cold-formed steel sections under gravity and lateral loads. Their investigations showed that using package and design studs based on capacity leads to increase shear strength.

So far, most research has been done on cross bracing systems; while little attention has been given to other bracing arrangements and evaluating their seismic behavior. Despite experiments and studies on cross bracing systems, there exist uncertainties about the exact nonlinear behavior of these systems. To shed light on this significant issue, using modeling, analysis by finite element method, and considering various ratios of height to length of the wall and evaluating nonlinear responses of these systems, we decided to investigate several bracing systems with different arrangements including cross, chevron and K-shape bracings.

Available design guidelines

AISI standards (2001a, b) as one of the pioneer centers working on CFS framing systems prescribe a range of R factors between 2 and 7 for different basic seismic force-

resisting system, though it emphasizes that some additional essential detailing is needed for $R > 3$.

ASCE7 (2005) stipulates that the design of lightweight cold-formed steel structures to resist seismic loads shall be in accordance with the requirements of AISI. However, it requires that for those systems, e.g., a K-braced system, which are not detailed in accordance with AISI, one shall use the R factor designated for "structural steel systems not specifically detailed for seismic resistance" which is equal to 3.

The American NEHRP recommends seismic provisions FEMA 450 (2003), FEMA P750 (2009) and the Technical Instructions, TI 809-07 (1998), specify that the seismic response modification factor of 4 for diagonal strapping system; for other steel systems such as K-braced configurations, the value of 3 is stipulated.

Also, the Australian cold-formed steel structures standard, AS/NZS 4600-05 (2005), requires that when cold-formed steel members are used as the primary earthquake-resisting element, the selected response modification factor shall not be greater than 2, unless specified otherwise.

A simple, but important conclusion from the above review is that there is not a universal agreement on the value of response modification factor, R, and in particular there is no reference in the codes specifically for the R factor of systems braced with K-braces. Therefore, more studies are required to clarify this matter.

Basic concepts

Investigating the parameters of nonlinear behavior and ductility is of utmost importance. These issues are addressed under the rubric of response modification factor.

Stiffness and strength

The position of the predicted strengths, S_{yn} and S_{yp}, with respect to S_y may vary from what is illustrated depending on the particular wall being analyzed. The predicted nominal lateral yield strength, S_{yn}, of the wall was based on the tension yield strength of the braces determined using their nominal area (width × thickness) as well as the minimum specified (nominal) yield stress. The nominal tension yield capacity of the brace was adjusted for the inclined position of the strap members with respect to the horizontal. The predicted nominal lateral shear stiffness of the wall, kN, was calculated based on the axial stiffness of the two tension brace members, which was also adjusted for their inclined position with respect to the horizontal. The predicted values S_{yn} and kN represent the nominal (not factored) design parameters that an engineer would typically be able to determine using minimum specified

member sizes and material properties without the aid of test results and measurements. S_{yp} is the predicted lateral yield strength of the wall, which is typically reached when the strap braces yield in tension. K_p is the predicted lateral shear stiffness of the wall, again obtained from the initial elastic axial stiffness of the strap braces alone. The maximum load level reached by each braced wall regardless of the failure mode was defined as the measured yield strength, S_y. The measured initial elastic shear stiffness K_e, was defined as the secant stiffness from the zero load level to the 40 % of maximum load level, $S_{0.4}$, as recommended in ASTM E2126 (2005) (Fig. 1).

Ductility

The main factor influencing the behavior factor is the ductility factor. Ductility is, in fact, the ability of bearing nonlinear displacements of the system, so that when the system reaches its yielding capacity, it can still withstand forces until it reaches substantially nonlinear lateral displacement without the structure being collapsed. The ductility of the system has been calculated according to the following equation:

$$\mu = \frac{\Delta_{0.8}}{\Delta_{syp}}. \tag{1}$$

In this equation, Δ_{syp}, is elastic yielding ductility calculated by measuring elastic stiffness (K_e) and lateral yielding wall resistance (S_{yp}). $\Delta_{0.8}$ is the rate of displacement failure continuing until there is no resistance (80 % of the ultimate resistance is reduced).

Response modification factor

The concept of response modification factor is based on the ductile behavior of the structure to absorb seismic energy as well as delay in structure failure. In fact, benefiting from the reality that any structure has a bit additional resistance and ductility, earthquake regulations allow designing structures with less power and they pay the fine of this reduction in force by accepting larger displacements. Research has shown that two factors of additional resistance factor (R_0) and force reduction factor have the greatest impact on the behavior factor at the non-elastic stage due to ductility (R_d). Behavior response modification factor is written as follows:

$$R = R_0 \times R_d. \tag{2}$$

Additional resistance factor (R_0) is the ratio of total yielding limit of structure during the formation of failure mechanism to force corresponding to the formation of the first plastic hinge:

Fig. 1 Measured and predicted wall strength and stiffness
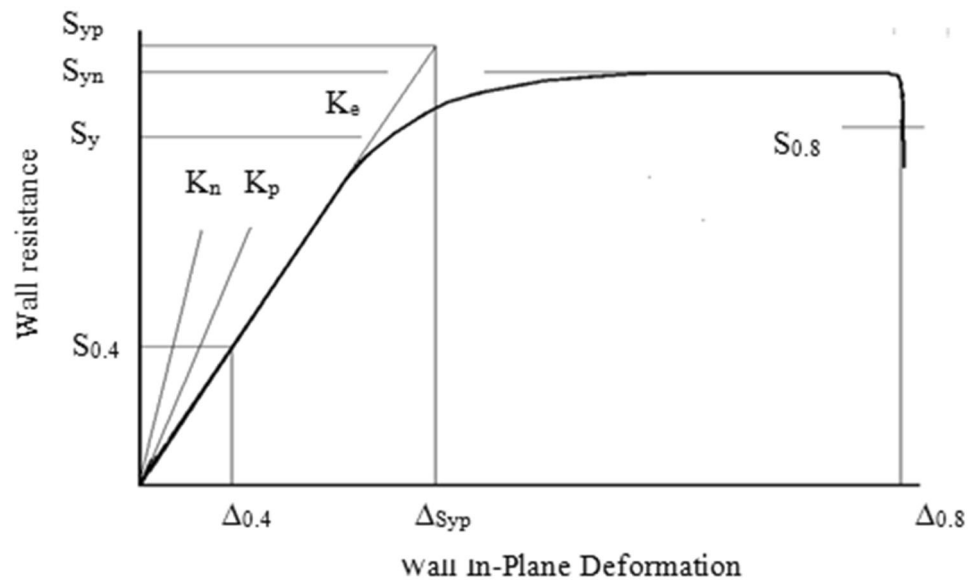
$$R_0 = \frac{S_y}{S_{yn}}. \tag{3}$$

To apply the effect of ductility factor parameter, a factor called force reduction factor due to ductility (R_d) has been introduced and when the fundamental period of the structure is between 0.1 and 0.5 s, Newmark and Hall (1982) force Equation is calculated as follows:

$$R_d = \sqrt{2\mu - 1}. \tag{4}$$

Modeling

In the present study, finite element numerical method was used to model the frames and evaluation of the nonlinear response of belt braces was applied as a lateral bracing system.

Validation of the analytical model with experimental model

One way to achieve higher confidence in all numerical modeling techniques is to adapt the numerical results with experimental ones. Hence, due to the similarity of the finite element model with the actual conditions, and the possibility of simulating the complexity of potential failure in members and connections and loading conditions, a reasonable model with the lowest error rate can be achieved. In estimating the monotonic behavior of cold-formed steel frames, LSF frame laboratory sample with tape cross brace by Al-Kharat and Rogers (2007) was used. Next, using finite element program and software MSC PATRAN-

NASTRAN (2012), it is modeled and the results of experimental analysis are compared.

The profiles of sections and materials used in the model

The sample test consisted of braced walls with crossed straps. The height and length of the frames were 2.44 m. Lateral studs made of double C-shaped sections were fused together from the front and the middle studs made of single C-shaped sections were installed with a nominal spacing of 406 mm. Modeling was performed using the same sections. Section profiles and behavior of materials used in double and single studs, tracks and belts are presented in Tables 1 and 2.

On the other hand, the walls comprised straps that were fillet welded to the gusset plates, which were in turn welded to the stud and track members. Also, flat plate hold downs were placed within the upper and lower tracks at the four corner locations of the wall (Fig. 2).

In terms of ductile seismic performance, the desirable mode of failure of a cold-formed steel braced wall system is generally that of gross cross section yielding of the straps, which form the fuse element in the SFRS. The other elements and connections in the seismic force-resisting system are expected to carry the force associated with the strap yielding load level. The strap braces should be able to enter into the inelastic range of behavior, such that ground motion-induced energy can be dissipated. Ideally, the braces would be able to maintain their yield capacity over extended lateral inelastic displacement of the wall without failure of the connections, gusset plates, tracks, chord studs or hold downs.

Table 1 Dimension sections and material properties

Member	Thickness (mm)	Dimensions (mm)	Nominal grade F_y (MPa)
Chord studs	1.91	152 × 41 × 12.7	345
Interior studs	1.22	152 × 41 × 12.7	230
Tracks	1.91	152 × 31.8	345
Strap bracing	1.91	152	230
Connection plate	1.91	300 × 300	230

Table 2 Matrix of strap-braced wall tests (nominal design dimensions and material properties)

Member	Nominal thickness (mm)	Thickness (mm)	Yield stress F_y (MPa)	Ultimate stress F_u (MPa)	F_u/F_y	Elng. (%)	F_y/F_{yn}
Chord studs	1.91	1.91	352	489	1.39	35	1.02
Interior studs	1.22	1.23	336	398	1.19	35	1.46
Tracks	1.91	1.94	348	474	1.36	37	1.01
Strap bracing	1.91	1.83	262	346	1.32	38	1.14

Fig. 2 Schematic drawing of heavy strap-braced test wall with corner detail
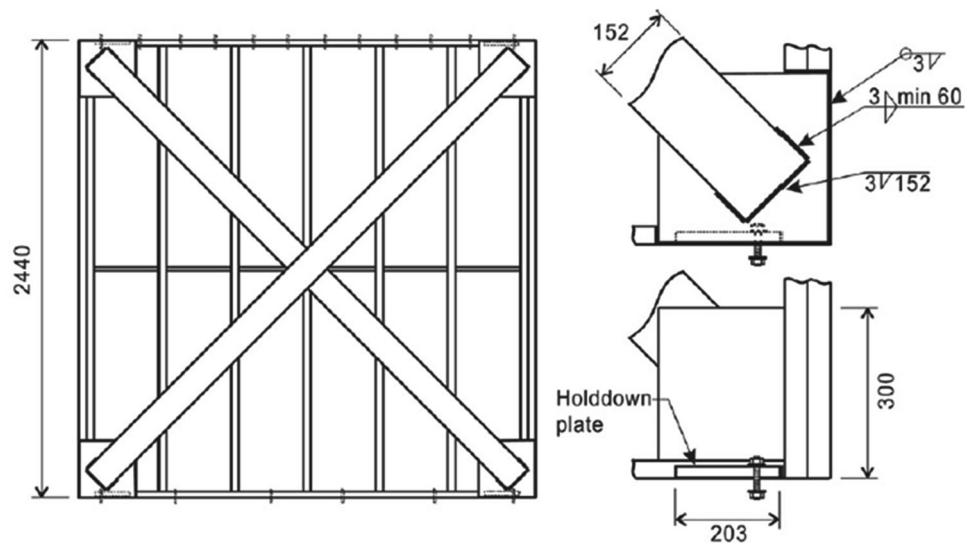
Components used in the analytical model

The basis of numerical finite element method which is used for solving a variety of engineering problems is the discretization of complex geometric models to easier and smaller elements to facilitate the analysis. The finite element model was formed by applying geometrical characteristics, mesh, material properties and supporting and loading conditions, and the geometry of frame was created by many surfaces of triangular and rectangular elements. For modeling the finite element, standard four-node elements (CQUAD 4) were used. To converge the analysis, the number of elements was selected in a way that a proper correspondence is established between the time of analysis and accuracy of the results.

The size of the selected meshes is equal to 20 mm. The structural model is appropriate for lightweight steel for precise and reliable prediction of the response of lightweight steel frames. In this study, a classical plasticity model of existing metals in software MSC PATRAN-NASTRAN for steel modeling was used. This model uses Von Mises yield surface with depending plastic flow which makes the isotropic yield possible. Using this model, there is the possibility of defining the behavior of complete plastic or isotropic hardening behavior or kinematics; in fact, steel hardening is a combination of isotropic and kinematic (compound) behaviors.

The type of lateral behavior analysis of the walls used is nonlinear pushover analysis. In this analysis, the stress–strain relationship is nonlinear and each point of sentences having the second derivative of ductility is also considered

in the strain calculation. So, the possibility of examining the behavior of the structure and ductility were calculated with higher accuracy.

Loading and support conditions

The cyclic loading regime that has been used in this study is based on Method B of ASTM Standard (2007), which was originally developed for ISO (International Organization for Standardization) standard 16670. This loading methodology consists of one full cycle at 0.5, 1, 2, 3 and 4 mm and three full cycles at 8, 16, 24, 32, 40, 48, 56, 64 and 72 mm, unless failure or a significant decrease in the load resistance occurs earlier. The mentioned lateral amplitudes correspond to 1.55, 3.125, 6.25, 9.35, 12.5, 25, 50, 75, 100, 125, 150, 175, 200 and 225 % of the ultimate monotonic lateral displacement of the walls, which was evaluated to be equal to 32 mm. It is worth noting that Method B of ASTM E2126-07 stipulates that the amplitude of cyclic displacements has to be selected based on fractions of monotonic ultimate displacement. If this was applied here, since each specimen had its own ultimate displacement, the loading regime would vary for different specimen types. However, as set out earlier, one of the current research objectives is the comparison of different types of K-braced configurations of the shear walls, which would necessitate using identical cyclic amplitudes for different walls. Hence, Method B is used in this study with lateral amplitude independent of monotonic testing. Moreover, although 75 mm, or 3.125 %, the inter-story drift ratio was the maximum amplitude of the actuator and was considered to be adequate, since the maximum allowable story drift ratio specified by the Standard FEMA450 (2003) is 2.5 %. The average loading velocity was about 2 mm/s which is compatible with the ASTM E2126-07 recommendation that the loading velocity must be in the range of 1–63 mm/s.

Results obtained from evaluating the validation of the modeling

The results from modeling by finite element software and laboratory work Al-Kharat and Rogers (2007)have been presented in Table 3 and Fig. 3. According to the results, a proper correspondence is observed between different parameters from numerical and experimental results of the samples. The difference less than 5 % causes an increased confidence in the obtained results in the evaluation.

All failure mechanisms of braced frames that occur in the laboratory cannot be seen in a finite element modeling. Therefore, some of the mechanisms of failure (belt buckling failure mode and overall deformation of the frame) are shown in Fig. 4.

Finite element modeling of Von Mises stress distribution at the end of the operation is shown in Fig. 5. The

Table 3 Comparison of results, experimental and analytical

Behavior	Specimen		
	Analytical	Experimental	Difference (%)
S_y (kN)	86.23	82.93	3.8
S_{yp}(kN)	108.17	103.40	4.6
K_e (kN/mm)	4.14	3.61	3.2
$\Delta_{0.8}$ (mm)	68.47	71.93	4.7
Energy (kN mm)	5819	5622	3.4

critical value of the stress field occurred at the end of the studs, which could damage the local buckling of the stud and make them unable to reach a total capacity of yield.

Parametric study

After ensuring the accuracy of the analytical model provided by experimental results, several frame samples with different brace arrangements including Chevron, cross and K-shape bracing were modeled in finite element software. The height of all frames was assumed to be fixed (2.44 m) and their length variable. Each frame consists of an upper and lower track, lateral and middle studs, and steel belt braces. Sections and materials used in studs, tracks and belts were the same in all samples and their characteristics have been presented in Tables 1 and 2.

Nine main types of frames were studied as shown in Fig. 6. Accordingly, in total, after modeling in finite element software under cyclic and monotonic loading, 68 frames were examined in this study.

Discussion on results

In this part, results of seismic parameters for each model and diagrams from cyclic and monotonic loading of each sample will be discussed. Values of (R_0) and (R_d) were calculated according to Eqs. (3, 4), respectively, and finally, for each sample, the values of response modification factor were calculated using Eq. (2).

Numerical analysis of frame of samples A

Under monotonic loading, the mean value of yielding capacity for these walls was equal to 6.07 kN that is equivalent to 78.36 % of the value of the predicted yielding capacity. Under cyclic loading, the mean yielding resistance was obtained as 6.29 kN and the ratio of (S_y/S_{yp}) was equal to 79.13 %. For monotonic and cyclic tests, the mean value of $\Delta_{0.8}$ was assessed as 119.83 and 124.91, respectively, and the mean value of ductility was equal to 4.39 and 4.97, respectively (Table 4).

Fig. 3 Comparison of results, experimental and analytical
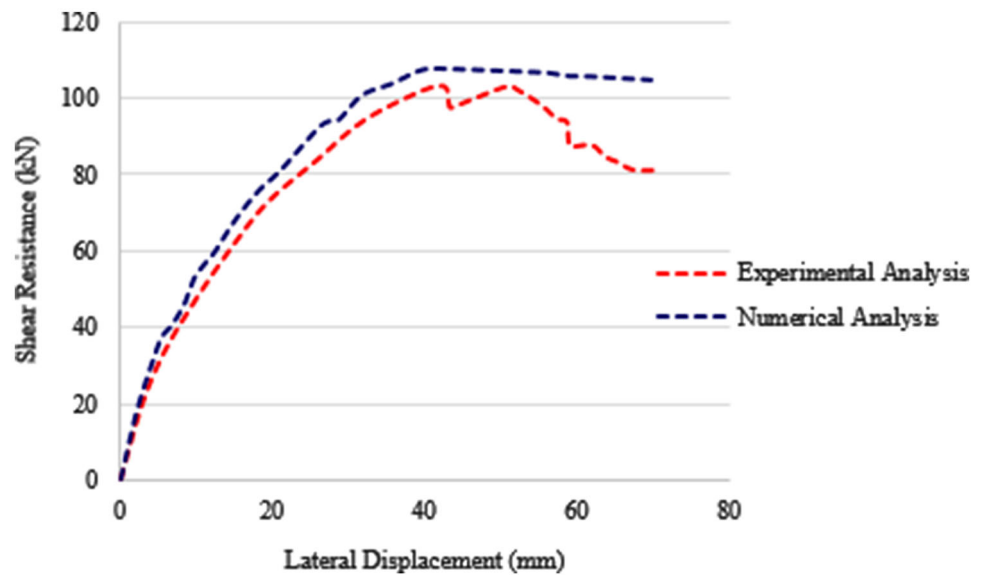
Fig. 4 Overall deformation of the frame: **a** experimental model, **b** analytical model (FEM)
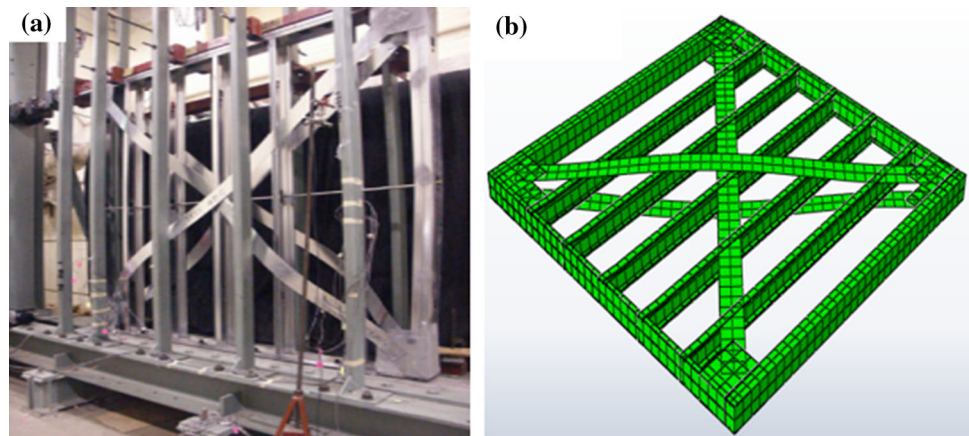
To calculate (R_d) from Eq. (3) for wall without brace, a value of mean ductility equal to 4.67 was used and the value of R_d was evaluated as 2.89 for walls without brace (Table 9). Since the value of (S_y/S_{yp}) is less than 1, there is no additional resistance; thus the value of (R_0) is considered equal to 1. Finally, the value of the response modification factor was obtained as 2.89 (Fig. 7).

By increasing the rate of height to length of wall, elastic stiffness and stiffness values are expected to increase and the amount of plasticity decreased. Using double straps will improve strength, stiffness and ductility.

Numerical analysis of frames of samples B

The mean value of yielding capacity under monotonic loading of sample B with lateral and bilateral braces was obtained as 106.64 and 169.53 kN, respectively, which has been predicted as being equivalent to 73.85 and 75.50 % of

the capacity values (Tables 5, 6). The mean value of yielding capacity under cyclic loading of samples B with lateral and bilateral braces was obtained as 114.80 and 183.58 kN, respectively, and also the ratio of (S_y/S_{yp}) was obtained as 73.24 and 135.91 % respectively (Tables 7, 8). The value of the yielding capacity of bilateral brace was around 60 % more than that of the lateral brace. Sample B with a lateral brace could not get the total of predicted yielding capacity and, at the moment of wall failure, the brace did not reach the total of its yielding capacity; however, the status of bilateral brace sample has somewhat improved compared to that of lateral brace sample and it could get the total of predicted capacity under cyclic loading.

For the ratio of yielding capacity to the nominal yielding capacity, the mean value was 101.56 and 161.64 % respectively (Tables 5, 6), under monotonic loading of these samples with lateral and bilateral braces and 109.33 and

Fig. 5 Von Mises stress distribution (FEM)
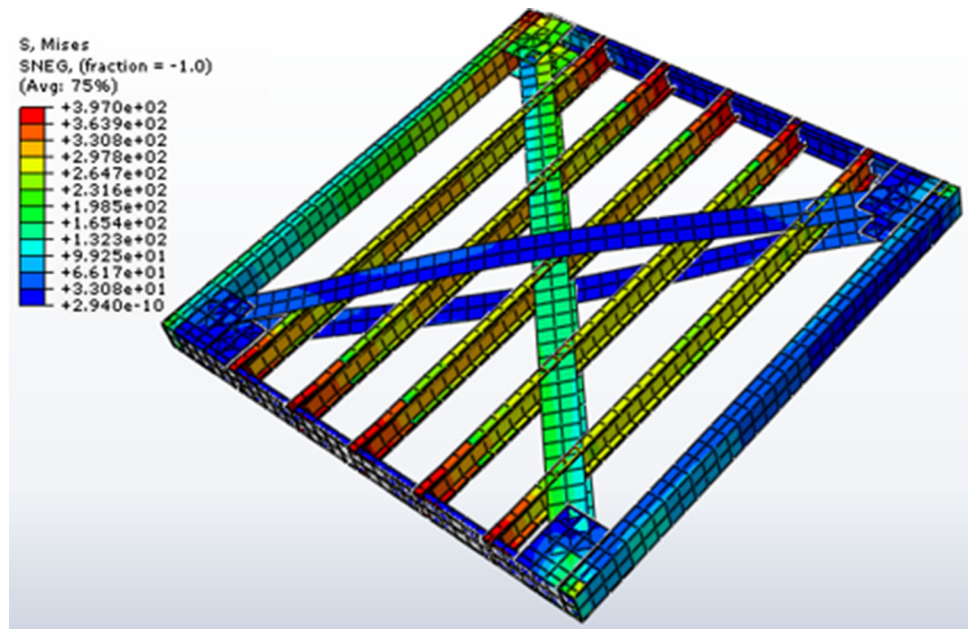
174.84 %, respectively, (Tables 7, 8) under cyclic loading. These values show that sample B with lateral and bilateral brace could get the expected nominal design shear resistance well.

The mean value of ($\Delta_{0.8}$) was evaluated as 45.51 and 43.24 mm, respectively (Tables 5, 6), under monotonic loading of samples B with lateral and bilateral braces and 44.41 and 42.93 mm, respectively (Tables 7, 8), under cyclic loading. The presence of bilateral brace on the wall causes about 4 % reduction in its maximum displacement compared to lateral brace samples. The mean value of ductility was evaluated as 2.02 and 2.27, respectively (Tables 5, 6), under monotonic loading of samples B with lateral and bilateral braces and 2.14 and 2.23, respectively (Tables 7, 8) under cyclic loading. To calculate (R_d) from Eq. (3) for wall with lateral brace, a mean value of ductility equal to 2.08 was used and the value of R_d was evaluated as 1.78. The mean value of additional resistance (R_0) was equal to 1.05 for wall with lateral brace and, finally, the value of the response modification factor was obtained as 1.87 (Table 9). To calculate the value of (R_d) for wall with bilateral brace, a mean value of ductility equal to 2.25 was used and the value of R_d was evaluated equal to 1.87. Based on values of (S_y/S_{yp}), the mean value of additional resistance (R_0) was equal to 1.68 for wall with bilateral brace and, finally, the value of the response modification factor was obtained as 3.14 for sample B with bilateral brace (Table 9). If the bilateral brace is used for sample B, the value of the response modification factor will be about 66 % more than that of the lateral brace.

By increasing the rate of height to length of the wall, elastic stiffness and stiffness values are expected to increase and the amount of plasticity decreased. Using double straps will improve strength, stiffness and ductility.

The value of predicted stiffness was obtained as 19.62 and 37.56 kN/mm, respectively, for samples B with lateral and bilateral braces under monotonic loading (Tables 5, 6) and 42.95 and 45.69 kN/mm, respectively, under cyclic loading (Tables 7, 8). Obviously, the value of (K_e) is considerably less than (K_p). The shear resistance is increased by increasing the ratio of the height to length of the wall. On the other hand, the shear wall resistance of the bilateral brace was significantly more than that of the lateral brace. This has been clearly shown in Fig. 8a–c.

## Numerical analysis of frames of samples C

The mean value of yielding capacity under monotonic loading of samples C with lateral and bilateral braces was obtained as 118.41 and 180.14 kN, respectively, which has been predicted as equivalent to 74.85 and 75.76 % of the capacity values (Tables 5, 6). The mean value of yielding capacity under cyclic loading of samples C with lateral and bilateral braces was obtained as 125.35 and 191.59 kN, respectively, and also the ratio of (S_y/S_{yp}) was obtained as 74.22 and 137.16 %, respectively (Tables 7, 8). The value of the yielding capacity of the bilateral brace was around 52 % more than that of the lateral brace. Sample C with a lateral brace could not get the total of predicted yielding capacity and at the moment of wall failure, braces did not reach the total of the yielding capacity; however, the status of bilateral brace sample has somewhat improved compared to that of the lateral brace sample and could obtain the total of the predicted capacity under cyclic loading. For

Fig. 6 General configuration of specimens
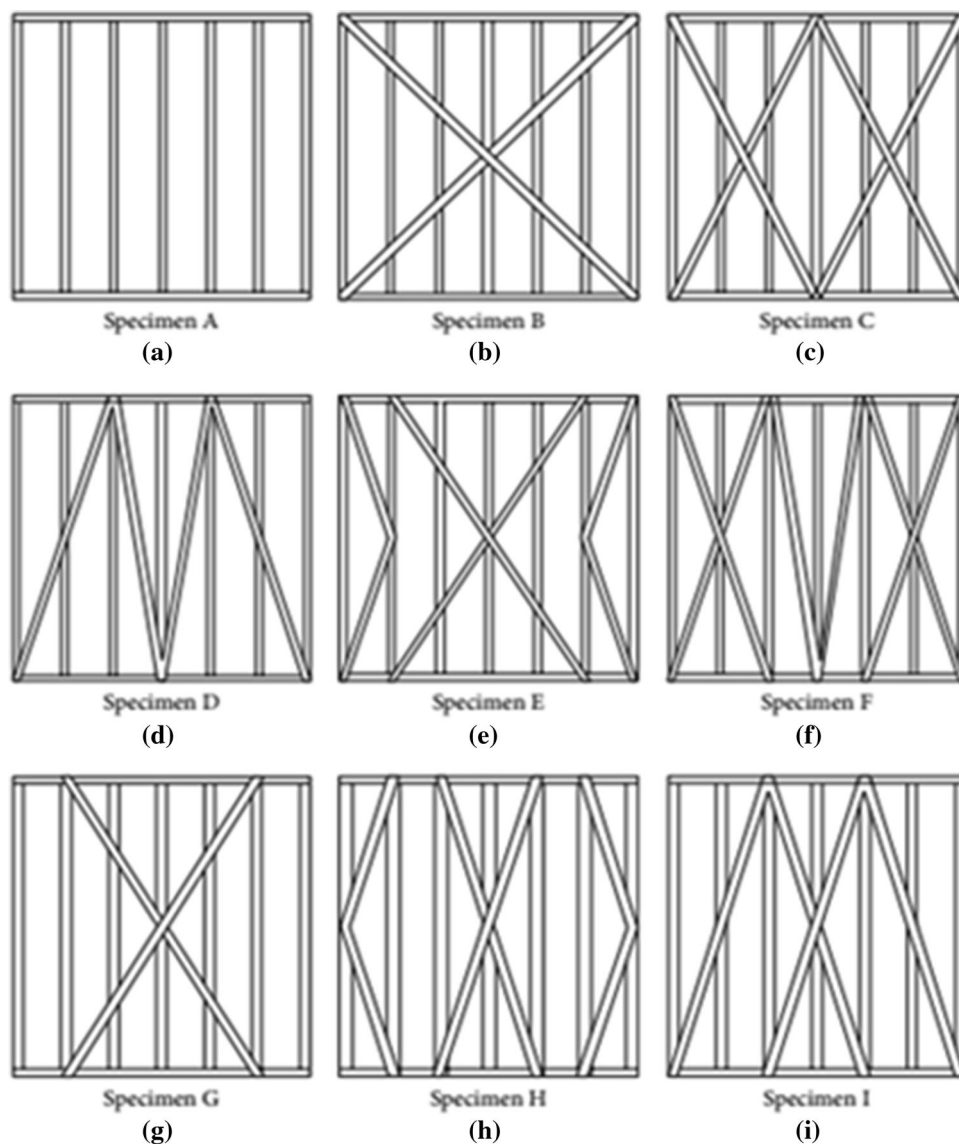
the ratio of yielding capacity to the nominal yielding capacity, the mean value was 112.77 and 171.56 %, respectively (Tables 5, 6), under monotonic loading of these samples with lateral and bilateral braces and 119.38 and 182.47 %, respectively (Tables 7, 8), under cyclic loading. These values show that sample C with lateral and bilateral brace could get the expected nominal design shear resistance well.

The mean value of ($\Delta_{0.8}$) was evaluated as 37.14 and 36.89 mm, respectively (Tables 5, 6), under monotonic loading of samples C with lateral and bilateral braces and 35.78 and 34.59 mm, respectively (Tables 7, 8), under cyclic loading. The presence of bilateral brace on the wall causes about 2 % reduction on its maximum displacement compared to lateral brace samples. The mean value of ductility was evaluated as 1.72 and 2.03, respectively

(Tables 5, 6), under monotonic loading of samples C with lateral and bilateral braces and 1.82 and 1.89, respectively (Tables 7, 8), under cyclic loading. To calculate (R_d) from Eq. (3) for wall with lateral brace, a mean value of ductility equal to 1.77 was used and the value of R_d was evaluated as 1.59. The mean value of additional resistance (R_0) was equal to 1.16 for wall with lateral brace and, finally, the value of the response modification factor was obtained as 1.85 (Table 9). To calculate the value of (R_d) for wall with bilateral brace, a mean value of ductility equal to 1.96 was used and the value of R_d was evaluated equal to 1.71. Based on values of (S_y/S_{yp}), the mean value of additional resistance (R_0) was equal to 1.77 for wall with bilateral brace and, finally, the value of the response modification factor was obtained as 3.02 for sample C with bilateral brace (Table 9). If the bilateral brace is used for sample C,

**Table 4** Loading results of lateral braced walls

Spec.	H/L	S_y (kN)	S_{yp} (kN)	K_e (kN/mm)	$\Delta_{0.8}$ (mm)	μ	Energy (kN mm)	K_p (kN/mm)	S_y/S_{yp} (%)	S_y/S_{yn} (%)	K_e/K_p (%)	K_e/K_n (%)
B	0.5	26.93	41.37	2.9	32.27	2.26	4097	4.62	65.1	25.65	62.68	16.55
	1	90.69	125.18	5.91	43.4	2.05	8186	15.21	72.45	86.37	38.88	33.79
	1.5	144.7	185.74	6.77	53.25	1.94	11631	25.65	77.9	137.81	26.38	38.67
	2	164.23	205.45	7.04	53.11	1.82	11,554	32.98	79.94	156.41	21.35	40.23
Avg		106.64	139.44	5.65	45.51	2.02	8867	19.62	73.85	101.56	37.32	32.31
SD		61.57	73.76	1.9	9.96	0.187	3562	12.37	–	–	–	–
Cov		0.577	0.529	0.366	0.219	0.093	0.402	0.631	–	–	–	–
C	0.5	28.26	42.06	3.21	22.57	1.72	2153	5.11	67.19	26.91	62.73	18.32
	1	93.68	130.15	6.15	38.28	1.81	8218	17.78	71.98	89.22	34.61	35.16
	1.5	170.3	205.82	8.09	44.79	1.76	13,739	31.47	82.74	162.19	25.7	46.21
	2	181.38	234.01	8.61	42.93	1.58	15,165	44.49	77.51	172.74	19.36	49.22
Avg		118.41	153.01	6.51	37.14	1.72	9118	24.71	74.85	112.77	35.6	37.23
SD		71.64	85.99	2.45	10.09	0.099	5923	17.02	–	–	–	–
Cov		0.605	0.562	0.376	0.272	0.058	0.603	0.689	–	–	–	–
D	0.5	11.65	20.56	1.14	54.24	3.01	1029	1.87	56.66	11.1	60.93	6.52
	1	33.37	50.66	2.18	68.47	2.95	2830	5.48	65.87	31.78	39.81	12.47
	1.5	77.25	105.8	3.52	84.96	2.83	6507	12.72	73.02	73.57	27.71	20.14
	2	125.43	151.23	4.87	85.16	2.74	9483	19.87	82.94	119.46	24.49	27.8
Avg		61.93	82.06	2.93	73.21	2.88	4962	9.99	69.62	58.98	38.24	16.73
SD		43.61	58.07	1.4	14.87	0.121	3778	7.99	–	–	–	–
Cov		0.704	0.708	0.478	0.203	0.042	0.762	0.8	–	–	–	–
E	0.5	19.76	30.5	1.9	34.28	2.41	1717	3.19	64.79	18.82	59.74	10.88
	1	64.78	81.64	3.87	49.59	2.35	5814	9.7	79.35	61.7	39.91	22.11
	1.5	138.29	162.31	6.01	61.31	2.27	11,502	22.11	85.2	131.7	27.18	34.34
	2	148.85	182.64	6.29	63.55	2.19	12,388	27.06	81.5	141.76	23.26	35.96
Avg		92.92	114.27	4.52	52.18	2.31	7855	15.51	77.71	88.5	37.52	25.82
SD		61.46	70.86	2.05	13.41	0.096	5022	10.99	–	–	–	–
Cov		0.661	0.62	0.454	0.257	0.042	0.639	0.709	–	–	–	–
F	0.5	24.52	37.36	2.48	35.29	2.34	1619	4.05	65.63	23.35	61.21	14.16
	1	66.56	85.94	4.28	45.4	2.26	4886	12.05	77.45	63.39	35.49	24.44
	1.5	139.87	168.45	6.47	56.77	2.18	10,824	24.24	83.03	133.21	26.69	36.97
	2	152.64	190.27	6.77	59.61	2.12	14,061	31.09	80.22	145.37	21.76	38.66
Avg		95.9	120.51	5	49.27	2.23	7847	17.86	76.58	91.33	36.29	28.56
SD		60.85	71.35	2.01	11.16	0.096	5628	12.11	–	–	–	–
Cov		0.635	0.592	0.403	0.227	0.043	0.717	0.678	–	–	–	–

Table 4 continued

Spec.	H/L	S_y (kN)	S_{yp} (kN)	K_e (kN/mm)	$\Delta_{0.8}$ (mm)	μ	Energy (kN mm)	K_p (kN/mm)	S_y/S_{yp} (%)	S_y/S_{yn} (%)	K_e/K_p (%)	K_e/K_n (%)
G	0.5	12.49	23.22	1.36	48.22	2.83	2459	2.24	53.79	11.9	60.74	7.79
	1	56.97	75.23	3.26	63.76	2.76	5093	8.15	75.73	54.26	39.96	18.61
	1.5	119.54	132.21	4.55	76.98	2.65	10,450	17.3	90.42	113.85	26.3	26.01
	2	143.93	163.45	5.43	76.4	2.54	10,941	25.03	88.06	137.08	21.71	31.05
	Avg	83.23	98.53	3.65	66.34	2.7	7235	13.18	77	79.27	37.18	20.86
	SD	59.71	62.08	1.77	13.53	0.127	4142	10.04	–	–	–	–
	Cov	0.717	0.63	0.484	0.204	0.047	0.572	0.762	–	–	–	–
H	0.5	12.67	17.79	0.98	60.39	3.34	775	1.58	71.22	12.07	62.11	5.62
	1	32.24	49.32	2.08	75.27	3.18	2908	4.87	65.37	30.7	74.75	11.91
	1.5	73.42	96.35	3.2	93.77	3.11	5911	9.9	76.2	69.92	32.27	18.26
	2	123.61	142.18	4.56	94.16	3.02	6965	16.83	86.94	117.72	27.1	26.06
	Avg	60.49	76.41	2.71	80.9	3.16	4139	8.3	74.93	57.6	41.06	15.46
	SD	49.11	54.45	1.53	16.27	0.135	2825	6.64	–	–	–	–
	Cov	0.812	0.713	0.566	0.201	0.043	0.683	0.8	–	–	–	–
I	0.5	13.16	24.65	1.53	41.19	2.56	1245	2.5	53.39	12.53	61.34	8.75
	1	57.65	79.02	3.59	54.66	2.48	4538	9.35	72.96	54.9	38.34	20.49
	1.5	128.68	151.64	5.4	67.7	2.41	9664	19.85	84.86	122.55	27.2	30.85
	2	145.36	165.74	5.7	67.47	2.32	10,826	26.6	87.7	138.44	21.42	32.57
	Avg	86.21	105.26	4.05	57.75	2.44	6568	14.58	74.73	82.11	37.08	23.16
	SD	61.79	65.82	1.92	12.61	0.102	4478	10.73	–	–	–	–
	Cov	0.717	0.625	0.474	0.218	0.042	0.682	0.736	–	–	–	–

H height of wall, L length of wall

Fig. 7 Curves of specimens A.
a Monotonic curves.
b Hysteretic envelope curve
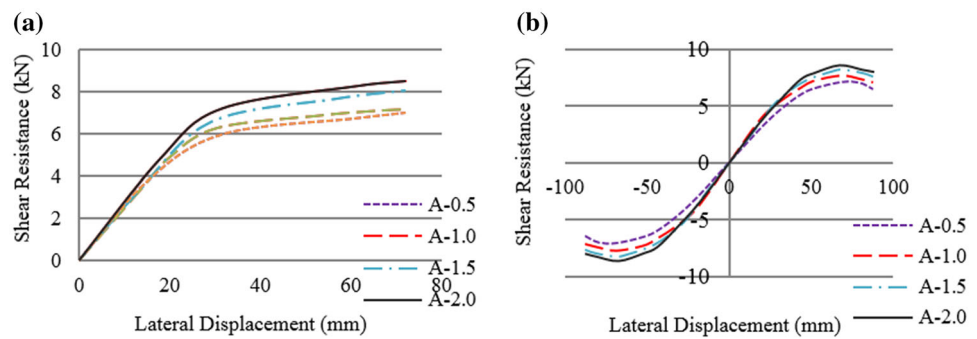
the value of the response modification factor will be about 63 % more than that of the lateral brace.

The value of predicted stiffness was obtained as 24.71 and 45.36 kN/mm, respectively, for samples C with lateral and bilateral braces under monotonic loading (Tables 5, 6) and 42.46 and 45.18 kN/mm, respectively under cyclic loading (Tables 7, 8). Obviously, the value of (K_e) is considerably less than (K_p). The shear resistance is increased by increasing the ratio of the height to length of the wall. On the other hand, the shear wall resistance of bilateral brace was significantly more than that of the lateral brace. This has been clearly shown in Fig. 9a–c.

Numerical analysis of frames of samples D

The mean value of yielding capacity under monotonic loading of samples D with lateral and bilateral braces was obtained as 61.93 and 87.11 kN, respectively, which has been predicted to be equivalent to 69.62 and 79.01 % of capacity values (Tables 5, 6). The mean value of yielding capacity under cyclic loading of samples D with lateral and bilateral braces was obtained as 69.13 and 96.02 kN, respectively, and also the ratio of (S_y/S_{yp}) was obtained as 74.27 and 120.70 %, respectively (Tables 7, 8). The value of the yielding capacity of bilateral brace was around 40 % more than that of the lateral brace. Sample D with a lateral brace could not get the total of predicted yielding capacity and, at the moment of wall failure, braces did not reach the total of the yielding capacity; however, the status of bilateral brace sample has somewhat improved compared to that of lateral brace sample and it could get the total of predicted capacity under cyclic loading. For the ratio of yielding capacity to the nominal yielding capacity, the mean value was 58.98 and 82.96 %, respectively (Tables 5, 6), under monotonic loading of these samples with lateral and bilateral braces and 65.84 and 91.44 %, respectively (Tables 7, 8), under cyclic loading. These values show that samples D with lateral and bilateral brace could not get the expected nominal design shear resistance.

The mean value of ($\Delta_{0.8}$) was evaluated as 73.21 and 55.31 mm, respectively (Tables 5, 6), under monotonic loading of samples D with lateral and bilateral braces and 71.49 and 69.11 mm, respectively (Tables 7, 8) under cyclic loading. The presence of bilateral brace on wall causes about 13.8 % reduction on its maximum displacement compared to the lateral brace samples. The mean value of ductility was evaluated as 2.88 and 2.97, respectively (Tables 5, 6), under monotonic loading of samples D with lateral and bilateral braces and 3.06 and 3.19, respectively (Tables 7, 8) under cyclic loading. To calculate (R_d) from Eq. (3) for wall with lateral brace, a mean value of ductility equal to 2.97 was used and the value of R_d was evaluated as 2.22. Since the value of (S_y/S_{yp}) is less than 1, there is no additional resistance; thus the value of (R_0) is considered equal to 1. Finally, the value of the response modification factor was obtained as 2.97 (Table 9). To calculate the value of (R_d) for wall with bilateral brace, a mean value of ductility equal to 3.08 was used and the value of R_d was evaluated equal to 2.27. Since the value of (S_y/S_{yp}) is less than 1, there is no additional resistance; thus the value of (R_0) is considered equal to 1. Finally, the value of the response modification factor was obtained as 2.27 for sample D with bilateral brace (Table 9). If the bilateral brace is used for sample D, the value of the response modification factor will be about 2.2 % more than that of lateral brace. This small difference can result from the lack of additional resistance in the samples.

The value of predicted stiffness was obtained as 9.99 and 19.37 kN/mm, respectively, for sample D with lateral and bilateral braces under monotonic loading (Tables 5, 6) and 14.95 and 15.91 kN/mm, respectively, under cyclic loading (Tables 7, 8). Obviously, the value of (K_e) is considerably less than (K_p). The shear resistance is increased by increasing the ratio of the height to length of the wall. On the other hand, the shear wall resistance of the bilateral brace was significantly more than the lateral brace. This has been clearly shown in Fig. 10a–c.

By increasing the rate of height to length of the wall, the elastic stiffness and stiffness values are expected to

Table 5 Monotonic loading results of bilateral braced walls

Spec.	H/L	S_y (kN)	S_{yp} (kN)	K_e (kN/mm)	$\Delta_{0.8}$ (mm)	μ	Energy (kN mm)	K_p (kN/mm)	S_y/S_{yp} (%)	S_y/S_{yn} (%)	K_e/K_p (%)	K_e/K_n (%)
B	0.5	78.34	108.24	9.02	29.28	2.44	8165	14.57	72.38	74.61	61.18	51.56
	1	161.1	220.82	12.42	42.29	2.38	14,054	32.72	72.96	153.43	37.95	70.96
	1.5	208.43	258.95	11.23	50.1	2.17	16,963	43.62	80.49	198.5	25.75	64.17
	2	230.26	302.28	12.33	51.3	2.09	18,810	59.17	76.17	219.3	20.84	70.47
Avg		169.53	222.57	11.25	43.24	2.27	14,498	37.56	75.5	161.46	36.43	64.29
SD		67.3	83.17	1.58	10.13	0.165	4653	18.69	–	–	–	–
Cov		0.397	0.374	0.14	0.234	0.073	0.321	0.497	–	–	–	–
C	0.5	82.13	112.13	10.17	22.94	2.08	4089	16.62	73.25	78.22	61.24	58.14
	1	192.31	241.56	13.6	36.66	2.06	14,654	40.24	79.61	183.15	33.79	77.7
	1.5	210.45	288.09	13.48	43.27	2.02	18,423	53.72	73.05	200.43	25.09	77.01
	2	235.66	305.6	13.39	44.71	1.96	19,577	70.85	77.11	224.44	18.9	76.51
Avg		180.14	236.85	12.66	36.89	2.03	14,185	45.36	75.76	171.56	34.75	72.34
SD		67.71	87.42	1.659	9.94	0.054	7051	22.89	–	–	–	–
Cov		0.376	0.369	0.131	0.27	0.027	0.497	0.505	–	–	–	–
D	0.5	21.98	32.6	2.57	38.89	3.07	1830	5.77	67.42	20.93	44.59	14.71
	1	72.78	95.21	5.64	50.78	3.01	5394	16.28	76.44	69.31	34.65	32.24
	1.5	122.12	140.23	6.41	65	2.97	10,879	24.61	87.09	116.3	26.05	36.63
	2	131.54	154.61	6.55	66.66	2.82	11,261	30.81	85.08	125.28	21.25	37.4
Avg		87.11	105.66	5.29	55.33	2.97	7341	19.37	79.01	82.96	31.63	30.25
SD		50.49	54.89	1.86	13.07	0.106	4547	10.84	–	–	–	–
Cov		0.58	0.519	0.351	0.236	0.036	0.619	0.56	–	–	–	–
E	0.5	32.63	50.98	3.36	41.6	2.74	2967	9.3	64.01	31.08	36.09	19.18
	1	124.58	158.67	7.98	50.46	2.54	10,335	19.12	78.52	118.65	41.74	45.6
	1.5	174.88	212.51	8.39	59.79	2.36	13,976	26.63	82.29	166.55	31.5	47.95
	2	177.48	225.18	8.6	59.65	2.28	14,038	32.5	78.82	169.03	26.46	49.13
Avg		127.39	161.84	7.08	52.88	2.48	10,329	21.89	75.91	121.33	33.95	40.47
SD		67.7	79.33	2.5	8.69	0.205	5204	10.02	–	–	–	–
Cov		0.531	0.49	0.353	0.164	0.083	0.504	0.458	–	–	–	–
F	0.5	39.83	54.95	4.08	34.95	2.6	2970	11.48	72.48	37.93	35.56	23.33
	1	127.43	162.06	9.14	43.26	2.44	9395	23.47	78.63	121.36	38.96	52.25
	1.5	198.47	251.07	11.07	50.94	2.25	15,924	41.71	79.05	189.02	26.53	63.23
	2	221.34	282.97	11.61	53.23	2.18	17,802	51.12	78.22	210.8	22.71	66.33
Avg		146.77	187.76	8.98	45.6	2.37	11,522	31.95	77.1	139.78	30.94	51.29
SD		81.74	102.26	3.43	8.28	0.189	6744	17.83	–	–	–	–
Cov		0.557	0.545	0.382	0.182	0.08	0.585	0.558	–	–	–	–

Table 5 continued

Spec.	H/L	S_y (kN)	S_{yp} (kN)	K_e (kN/mm)	$\Delta_{0.8}$ (mm)	μ	Energy (kN mm)	K_p (kN/mm)	S_y/S_{yp} (%)	S_y/S_{yn} (%)	K_e/K_p (%)	K_e/K_n (%)
G	0.5	23.46	42.13	2.94	43.75	3.06	4863	7.45	55.68	22.34	39.53	16.82
	1	83.14	110.06	5.67	53.56	2.76	9406	14.54	75.54	79.18	39.01	32.41
	1.5	134.51	151.06	6.19	64.67	2.65	11,690	24.11	89.04	128.1	25.67	35.37
	2	142.18	161.34	6.39	64.18	2.54	11,933	30.13	88.12	135.41	21.19	36.49
Avg		95.82	116.15	5.3	56.54	2.75	9473	19.06	77.1	91.26	31.35	30.27
SD		54.9	54.09	1.6	9.95	0.222	3277	10.06	–	–	–	–
Cov		0.573	0.466	0.302	0.176	0.081	0.346	0.528	–	–	–	–
H	0.5	19.68	28.16	1.33	71.59	3.39	2346	5.23	69.89	18.74	25.47	7.62
	1	70.06	92.14	4.15	72.07	3.24	5775	17	76.04	66.72	24.4	23.7
	1.5	118.54	132.74	5.67	73.75	3.15	10,654	21.22	89.3	112.9	26.73	32.4
	2	124.68	152.08	6.05	78.15	3.11	11,708	21.57	81.98	118.74	28.07	34.59
Avg		83.24	101.28	4.3	73.89	3.22	7620	16.25	79.3	79.28	26.17	24.58
SD		48.91	54.77	2.14	2.99	0.124	4364	7.63	–	–	–	–
Cov		0.588	0.541	0.498	0.04	0.039	0.573	0.47	–	–	–	–
I	0.5	26.74	44.58	2.95	41.85	2.76	2266	8.02	59.98	25.47	36.72	16.83
	1	121.5	149.42	7.66	50.93	2.61	8657	19.72	81.31	115.71	38.86	43.79
	1.5	138.71	162.74	6.45	60.77	2.41	10,908	23.85	85.23	132.1	27.05	36.88
	2	147.49	166.5	6.38	60.57	2.32	11,210	26.68	88.58	140.47	23.9	36.44
Avg		108.61	130.81	5.86	53.53	2.53	8260	19.57	78.78	103.44	31.63	33.49
SD		55.64	57.95	2.03	9.04	0.2	4155	8.21	–	–	–	–
Cov		0.512	0.443	0.347	0.169	0.079	0.503	0.42	–	–	–	–

H height of wall, L length of wall

Table 6 Cyclic loading results of lateral braced walls

Spec.	H/L	S_y (kN)	S_{yp} (kN)	K_e (kN/mm)	$\Delta_{0.8}$ (mm)	μ	Energy (kN mm)	K_p (kN/mm)	S_y/S_{yp} (%)	S_y/S_{yn} (%)	K_e/K_p (%)	K_e/K_n (%)
B	0.5	29.75	42.94	3.27	31.53	2.40	4782	9.63	69.28	28.33	33.95	18.68
	1	96.63	137.35	7.05	42.26	2.17	17,998	33.75	70.35	92.03	20.9	40.3
	1.5	152.32	195.64	7.75	52.02	2.06	26,658	53.89	77.86	145.07	14.37	44.27
	2	180.5	239.19	8.91	51.81	1.93	28,130	74.51	75.46	171.9	11.96	50.91
Avg		114.8	153.78	6.74	44.41	2.14	19,392	42.95	73.24	109.33	20.29	38.54
SD		66.55	84.86	2.44	9.72	0.199	10,716	27.76	–	–	–	–
Cov		0.58	0.552	0.362	0.219	0.093	0.553	0.646	–	–	–	–
C	0.5	30.76	44.36	3.67	23.46	1.94	5688	11.03	69.34	29.29	33.3	21
	1	98.64	139.41	7.16	36.99	1.9	18,586	35.29	70.75	93.94	20.3	40.94
	1.5	181.5	222.54	9.5	40.74	1.74	29,658	57.06	81.56	172.86	16.66	54.31
	2	190.51	253.25	10.13	41.94	1.68	33,016	66.47	75.23	181.44	15.24	57.89
Avg		125.35	164.89	7.62	35.78	1.82	21,737	42.46	74.22	119.38	21.38	43.54
SD		75.41	93.64	3.19	8.62	0.127	12,348	24.69	–	–	–	–
Cov		0.602	0.568	0.419	0.241	0.07	0.568	0.581	–	–	–	–
D	0.5	12.69	21.08	1.27	52.88	3.19	2286	2.66	60.2	12.09	47.71	7.27
	1	38.2	53.21	2.49	66.84	3.13	8212	7.56	71.79	36.38	32.97	14.24
	1.5	87.75	112.81	4.08	83.02	3	17,134	18.43	77.79	83.57	22.16	23.34
	2	137.89	157.96	5.52	83.21	2.91	23,580	31.16	87.29	131.32	17.73	31.57
Avg		69.13	86.27	3.34	71.49	3.06	12,803	14.95	74.27	65.84	30.14	19.1
SD		48	61.06	1.61	14.58	0.125	9426	12.65	–	–	–	–
Cov		0.694	0.708	0.482	0.204	0.041	0.736	0.846	–	–	–	–
E	0.5	21.08	32.42	2.2	37.29	2.53	4164	5.11	65.02	20.08	43.02	12.57
	1	70.43	101.68	5.24	48.34	2.49	12,706	19.04	69.27	67.08	27.51	29.93
	1.5	137.12	177.83	7.16	59.89	2.41	23,968	41.94	77.11	130.59	17.06	40.89
	2	160.18	208.58	7.81	58.47	2.19	26,374	56.22	76.79	152.55	13.9	44.64
Avg		97.2	130.13	5.6	51	2.41	16,803	30.58	72.05	92.57	25.37	32
SD		63.43	79.13	2.52	10.49	0.152	10,319	22.86	–	–	–	–
Cov		0.653	0.608	0.449	0.206	0.063	0.614	0.748	–	–	–	–
F	0.5	23.25	35.42	2.55	34.41	2.48	4212	6.66	65.64	22.14	38.35	14.59
	1	78.81	97.45	5.27	44.36	2.4	14,592	19.26	80.87	75.06	27.38	30.13
	1.5	150.24	181.56	7.58	55.34	2.31	25,838	43.43	82.75	143.09	17.45	43.31
	2	176.38	229.65	8.88	58.21	2.25	27,364	68.76	76.8	167.98	12.91	50.72
Avg		107.17	136.02	6.07	48.08	2.36	18,001	34.53	76.52	102.07	24.02	34.69
SD		69.5	86.5	2.78	10.89	0.101	10,814	27.45	–	–	–	–
Cov		0.649	0.636	0.458	0.227	0.043	0.601	0.795	–	–	–	–

Table 6 continued

Spec.	H/L	S_y (kN)	S_{yp} (kN)	K_e (kN/mm)	$\Delta_{0.8}$ (mm)	μ	Energy (kN mm)	K_p (kN/mm)	S_y/S_{yp} (%)	S_y/S_{yn} (%)	K_e/K_p (%)	K_e/K_n (%)
G	0.5	13.33	25.18	1.61	47.12	3.01	2760	3.21	52.94	12.7	50.01	9.18
	1	59.8	82.76	3.89	62.27	2.93	12,038	11.87	72.26	56.95	32.8	22.25
	1.5	126.36	151.2	5.66	70.82	2.65	23,008	25.89	83.57	120.34	21.85	32.33
	2	149.19	172.16	6.22	74.44	2.69	24,320	32.24	86.66	142.09	19.3	35.55
Avg		87.17	107.83	4.34	63.66	2.82	15,531	18.3	73.86	83.02	30.99	24.83
SD		62.14	67.03	2.08	12.15	0.176	10,140	13.18	–	–	–	–
Cov		0.713	0.622	0.478	0.191	0.062	0.653	0.72	–	–	–	–
H	0.5	11.07	20.13	1.21	58.88	3.54	2190	2.48	54.99	10.54	48.76	6.92
	1	36.56	50.08	2.3	73.39	3.37	7580	6.29	73	34.82	36.55	13.14
	1.5	78.58	109.32	3.94	91.54	3.3	16,814	14.23	71.88	74.84	27.69	22.52
	2	131.39	149.79	5.22	91.79	3.2	19,184	21.13	87.72	125.13	24.72	29.84
Avg		64.4	82.33	3.17	78.9	3.35	11,442	11.03	71.9	61.33	34.43	18.1
SD		52.62	58.28	1.77	15.88	0.143	7944	8.32	–	–	–	–
Cov		0.817	0.708	0.559	0.201	0.043	0.694	0.754	–	–	–	–
I	0.5	14.64	26.29	1.78	40.26	2.72	2982	3.65	55.69	13.94	48.64	10.15
	1	64.81	87.9	4.34	53.33	2.63	12,388	12.76	73.73	61.72	33.98	24.77
	1.5	135.97	163.92	6.34	66.16	2.56	23,616	28.61	82.95	129.5	22.17	36.25
	2	152.05	176.14	6.58	65.95	2.47	25,908	38.13	86.32	144.81	17.27	37.62
Avg		91.87	113.56	4.76	56.42	2.59	16,223	20.79	74.67	87.49	30.52	27.2
SD		63.93	70.06	2.23	12.33	0.108	10,622	15.49	–	–	–	–
Cov		0.696	0.617	0.469	0.219	0.042	0.655	0.745	–	–	–	–

H height of wall, *L* length of wall

Table 7 Cyclic loading results of bilateral braced walls

Spec.	H/L	S_y (kN)	S_{yp} (kN)	K_e (kN/mm)	$\Delta_{0.8}$ (mm)	μ	Energy (kN mm)	K_p (kN/mm)	S_y/S_{yp} (%)	S_y/S_{yn} (%)	K_e/K_p (%)	K_e/K_n (%)
B	0.5	84.77	42.94	3.52	30.48	2.5	7631	10.24	197.41	80.73	34.41	20.14
	1	174.25	137.35	7.6	40.86	2.26	33,650	35.9	126.87	165.95	21.18	43.45
	1.5	221.99	195.64	8.35	50.29	2.15	38,030	57.34	113.47	211.42	14.57	47.73
	2	253.32	239.19	9.61	50.09	2.01	42,453	79.27	105.91	241.26	12.12	54.89
Avg		183.58	153.78	7.27	42.93	2.23	30,441	45.69	135.91	174.84	20.57	41.55
SD		73.46	84.86	2.63	9.39	0.208	15,625.57	29.53	—	—	—	—
Cov		0.4	0.552	0.362	0.219	0.093	0.513	0.646	—	—	—	—
C	0.5	91.33	44.36	3.96	22.68	2.03	9055	11.74	205.88	86.98	33.75	22.64
	1	198.24	139.41	7.72	35.76	1.98	34,812	37.55	142.2	188.8	20.57	44.14
	1.5	225.31	222.54	10.25	39.39	1.81	40,048	60.7	101.24	214.58	16.88	58.56
	2	251.49	253.25	10.92	40.55	1.75	45,196	70.71	99.31	239.51	15.45	62.42
Avg		191.59	164.89	8.21	34.59	1.89	32,277.75	45.18	137.16	182.47	21.66	46.94
SD		70.29	93.64	3.15	8.2	0.132	16,051.76	26.26	—	—	—	—
Cov		0.367	0.568	0.384	0.237	0.07	0.497	0.581	—	—	—	—
D	0.5	24.51	21.08	1.37	51.13	3.32	3576	2.84	116.27	23.34	48.36	7.83
	1	84.93	53.21	2.69	64.61	3.26	14,686	8.04	159.61	80.89	33.41	15.35
	1.5	130.5	112.81	4.4	80.26	3.13	23,495	19.61	115.68	124.29	22.46	25.17
	2	144.13	157.96	5.96	80.44	3.03	26,575	33.14	91.24	137.27	17.97	34.04
Avg		96.02	86.27	3.6	69.11	3.19	17,083	15.91	120.7	91.44	30.55	20.6
SD		53.98	61.06	2	14.1	0.131	10,318.21	13.46	—	—	—	—
Cov		0.562	0.708	0.555	0.204	0.041	0.604	0.846	—	—	—	—
E	0.5	37.41	32.42	2.37	36.05	2.64	5534	5.44	115.39	35.63	43.6	13.55
	1	131.8	101.68	5.65	46.73	2.6	25,620	20.26	129.62	125.52	27.88	32.27
	1.5	179.19	177.83	7.72	57.89	2.51	31,798	44.62	100.76	170.66	17.29	44.09
	2	192.48	208.58	8.42	56.52	2.28	33,382	59.81	92.28	183.31	14.08	48.13
Avg		135.22	130.13	6.04	49.3	2.51	24,083.5	32.53	109.52	128.78	25.71	34.51
SD		70.22	79.13	2.71	10.14	0.158	12,811.72	24.32	—	—	—	—
Cov		0.519	0.608	0.449	0.206	0.063	0.532	0.748	—	—	—	—
F	0.5	46.9	35.42	2.75	33.26	2.58	5674	7.08	132.41	44.67	38.86	15.73
	1	135.41	97.45	5.68	42.88	2.5	28,017	20.49	138.95	128.96	27.75	32.48
	1.5	211.23	181.56	8.17	53.5	2.41	32,934	46.21	116.34	201.17	17.68	46.69
	2	237.51	229.65	9.57	56.27	2.35	36,751	73.15	103.42	226.2	13.08	54.69
Avg		157.76	136.02	6.54	46.48	2.46	25,844	36.73	122.78	150.25	24.34	37.4
SD		85.65	86.5	3	10.53	0.105	13,913.8	29.21	—	—	—	—
Cov		0.543	0.636	0.458	0.227	0.043	0.538	0.795	—	—	—	—

Table 7 continued

Spec.	H/L	S_y (kN)	S_{yp} (kN)	K_e (kN/mm)	$\Delta_{0.8}$ (mm)	μ	Energy (kN mm)	K_p (kN/mm)	S_y/S_{yp} (%)	S_y/S_{yn} (%)	K_e/K_p (%)	K_e/K_n (%)
G	0.5	26.74	25.18	1.73	45.56	3.13	4238	3.42	106.2	25.47	50.68	9.9
	1	91.82	82.76	4.2	60.2	3.05	21,919	12.63	110.95	87.45	33.24	23.99
	1.5	141.76	151.2	6.1	68.47	2.76	24,532	27.54	93.76	135.01	22.15	34.86
	2	158.58	172.16	6.71	71.97	2.8	28,994	34.3	92.11	151.03	19.56	38.33
Avg		104.73	107.83	4.68	61.55	2.94	19,920.75	19.47	100.75	99.74	31.41	26.77
SD		59.22	67.03	2.24	11.75	0.183	10,855.55	14.02	–	–	–	–
Cov		0.565	0.622	0.478	0.191	0.062	0.545	0.72	–	–	–	–
H	0.5	21.17	20.13	1.3	56.92	3.69	3150	2.64	105.17	20.16	49.41	7.46
	1	74.29	50.08	2.48	70.95	3.51	13,923	6.69	148.34	70.75	37.05	14.17
	1.5	123.19	109.32	4.25	88.49	3.44	21,772	15.14	112.69	117.32	28.06	24.28
	2	138.87	149.79	5.63	88.74	3.34	24,719	22.48	92.71	132.26	25.05	32.17
Avg		89.38	82.33	3.42	76.27	3.49	15,891	11.74	114.73	85.12	34.89	19.52
SD		53.14	58.28	1.91	15.36	0.149	9638.91	8.85	–	–	–	–
Cov		0.595	0.708	0.559	0.201	0.043	0.607	0.754	–	–	–	–
I	0.5	32.02	26.29	1.91	38.92	2.84	4934	3.88	121.8	30.5	49.29	10.94
	1	128.49	87.9	4.67	51.55	2.74	24,712	13.57	146.18	122.37	34.44	26.71
	1.5	142.98	163.92	6.84	63.96	2.67	26,984	30.43	87.23	136.17	22.47	39.08
	2	164.17	176.14	7.1	63.75	2.57	29,460	40.56	93.2	156.35	17.5	40.56
Avg		116.92	113.56	5.13	54.55	2.7	21,522.5	22.11	112.1	111.35	30.93	29.32
SD		58.46	70.06	2.4	11.92	0.113	11,227.69	16.48	–	–	–	–
Cov		0.5	0.617	0.469	0.219	0.042	0.522	0.745	–	–	–	–

H height of wall, L length of wall

Table 8 Monotonic and cyclic loading specimens of A results

Spec.	H/L	S_y (kN)	S_{yp} (kN)	K_e (kN/mm)	$\Delta_{0.8}$ (mm)	μ	Energy (kN mm)	K_p (kN/mm)	S_y/S_{yp} (%)	S_y/S_{yn} (%)	K_e/K_p (%)	K_e/K_n (%)
Monotonic	0.5	4.92	7.08	0.28	114.89	4.57	145.84	1.08	69.49	4.69	26.09	1.61
	1	5.6	7.2	0.27	116.91	4.42	157.77	1.09	77.78	5.33	24.99	1.56
	1.5	6.27	8.13	0.29	120.12	4.31	206.23	1.07	77.12	5.97	27.38	1.67
	2	7.47	8.39	0.28	127.42	4.26	236.48	0.98	89.03	7.11	28.75	1.6
Avg		6.07	7.7	0.28	119.83	4.39	186.58	1.05	78.36	5.78	26.8	1.61
SD		1.09	0.657	0.008	5.49	0.137	42.29	0.052	–	–	–	–
Cov		0.18	0.085	0.029	0.046	0.031	0.227	0.05	–	–	–	–
Cyclic	0.5	5.23	7.03	0.304	118.19	5.11	344	0.643	74.39	4.98	47.3	1.74
	1	5.84	7.56	0.311	122.16	5.02	376	0.753	77.25	5.56	41.26	1.78
	1.5	6.24	8.45	0.33	126.66	4.94	494	0.894	75.98	6.11	36.86	1.88
	2	7.68	8.64	0.314	132.63	4.82	568	0.938	88.89	7.31	33.47	1.79
Avg		6.29	7.92	0.315	124.91	4.97	445.5	0.807	79.13	5.99	39.72	1.8
SD		1.04	0.757	0.011	6.2	0.123	104.07	0.135	–	–	–	–
Cov		0.17	0.096	0.035	0.05	0.025	0.234	0.167	–	–	–	–

H height of wall, *L* length of wall

increase and the amount of plasticity decreased. Using double straps will improve strength, stiffness and ductility.

Numerical analysis of frames of samples E

The mean value of yielding capacity under monotonic loading of samples E with lateral and bilateral braces was obtained as 92.92 and 127.39 kN, respectively, which has been predicted equivalent to 77.71 and 75.91 % of the capacity values (Tables 5, 6). The mean value of yielding capacity under cyclic loading of samples E with lateral and bilateral braces was obtained as 97.20 and 135.22 kN, respectively, and also the ratio of (S_y/S_{yp}) was obtained as 72.05 and 109.52 %, respectively (Tables 7, 8). The value of the yielding capacity of bilateral brace was around 38 % more than that of the lateral brace. Sample E with a lateral brace could not get the total of predicted yielding capacity and at the moment of wall failure, braces did not reach the total of its yielding capacity; however, the status of bilateral brace sample has somewhat improved compared to that of the lateral brace sample and it could get the total of predicted capacity under cyclic loading. For the ratio of yielding capacity to the nominal yielding capacity, the mean value was 88.50 and 121.33 %, respectively (Tables 5, 6), under monotonic loading of these samples with lateral and bilateral braces and 92.57 and 128.78 %, respectively (Tables 7, 8), under cyclic loading. These values show that sample E with bilateral brace could get the expected nominal design shear resistance well.

The mean value of ($\Delta_{0.8}$) was evaluated as 52.18 and 52.88 mm, respectively (Tables 5, 6), under monotonic loading of samples E with lateral and bilateral braces and 51 and 49.30 mm, respectively (Tables 7, 8), under cyclic loading. The mean value of ductility was evaluated as 2.31 and 2.48, respectively (Tables 5, 6), under monotonic loading of samples E with lateral and bilateral braces and 2.41 and 2.51, respectively (Tables 7, 8) under cyclic loading. To calculate (R_d) from Eq. (3) for wall with lateral brace, a mean value of ductility equal to 2.36 was used and the value of R_d was evaluated as 1.93. Since the value of (S_y/S_{yp}) is less than 1, there is no additional resistance; thus the value of (R_0) is considered equal to 1. Finally, the value of the response modification factor was obtained as 1.93 (Table 9). To calculate the value of (R_d) for wall with bilateral brace, a mean value of ductility equal to 2.50 was used and the value of R_d was evaluated equal to 2. Based on values of (S_y/S_{yp}), the mean value of additional resistance (R_0) was equal to 1.25 for wall with bilateral brace and, finally, the value of the response modification factor was obtained as 2.50 for sample E with bilateral brace (Table 9). If the bilateral brace is used for sample E, the value of the response modification factor will be about 29.50 % more than that of lateral brace.

The value of predicted stiffness was obtained as 15.51 and 21.89 kN/mm, respectively, for samples E with lateral and bilateral braces under monotonic loading (Tables 5, 6) and 30.58 and 32.53 kN/mm, respectively, under cyclic loading (Tables 7, 8). Obviously, the value of (K_e) is considerably less than (K_p). The shear resistance is increased by increasing the ratio of the height to length of the wall. On the other hand, the shear wall resistance of the bilateral brace was significantly more than the lateral brace. This has been clearly shown in Fig. 11a–c.

Table 9 The evaluated seismic parameters

Specimen	Behavior			
	μ	R_d	R_o	R
A				
Without brace	4.68	2.89	1	2.89
B				
Lateral brace	2.08	1.78	1.05	1.87
Bilateral brace	2.25	1.87	1.68	3.14
C				
Lateral brace	1.77	1.59	1.16	1.85
Bilateral brace	1.96	1.71	1.77	3.02
D				
Lateral brace	2.97	2.22	1	2.22
Bilateral brace	3.08	2.27	1	2.27
E				
Lateral brace	2.36	1.93	1	1.93
Bilateral brace	2.5	2	1.25	2.5
F				
Lateral brace	2.3	1.89	1	1.89
Bilateral brace	2.42	1.96	1.45	2.84
G				
Lateral brace	2.74	2.13	1	2.13
Bilateral brace	2.85	2.17	1	2.17
H				
Lateral brace	3.26	2.35	1	2.35
Bilateral brace	3.36	2.39	1	2.39
I				
Lateral brace	2.52	2.01	1	2.01
Bilateral brace	2.62	2.06	1.07	2.2

Numerical analysis of frames of samples F

The mean value of yielding capacity under monotonic loading of samples F with lateral and bilateral braces was obtained as 95.90 and 146.77 kN, respectively, which has been predicted equivalent to 76.58 and 77.10 % of capacity values (Tables 5, 6). The mean value of yielding capacity under cyclic loading of samples F with lateral and bilateral braces was obtained as 107.17 and 157.76 kN, respectively, and also the ratio of (S_y/S_{yp}) was obtained as 76.52 and 122.78 %, respectively (Tables 7, 8). The value of the yielding capacity of bilateral brace was around 50 % more than that of the lateral brace. Sample F with a lateral brace could not get the total of predicted yielding capacity and, at the moment of wall failure, braces did not reach the total of the yielding capacity; however, the status of bilateral brace sample has somewhat improved compared to that of the lateral brace sample and it could get the total of predicted capacity under cyclic loading. For the ratio of yielding capacity to the nominal yielding capacity, the mean value was 91.33 and 139.78 %, respectively (Tables 5, 6), under monotonic loading of these samples with lateral and bilateral braces and 102.07 and 150.25 %, respectively (Tables 7, 8), under cyclic loading. These values show that sample F with bilateral brace could get the expected nominal design shear resistance well.

The mean value of $(\Delta_{0.8})$ was evaluated as 49.27 and 45.60 mm, respectively (Tables 5, 6), under monotonic loading of samples F with lateral and bilateral braces and 48.08 and 46.48 mm, respectively (Tables 7, 8), under cyclic loading. The presence of bilateral brace on wall

Fig. 8 Curves of specimens B. **a** Monotonic curves. **b** Hysteretic envelope curves, 1-side. **c** Hysteretic envelope curves, 2-side
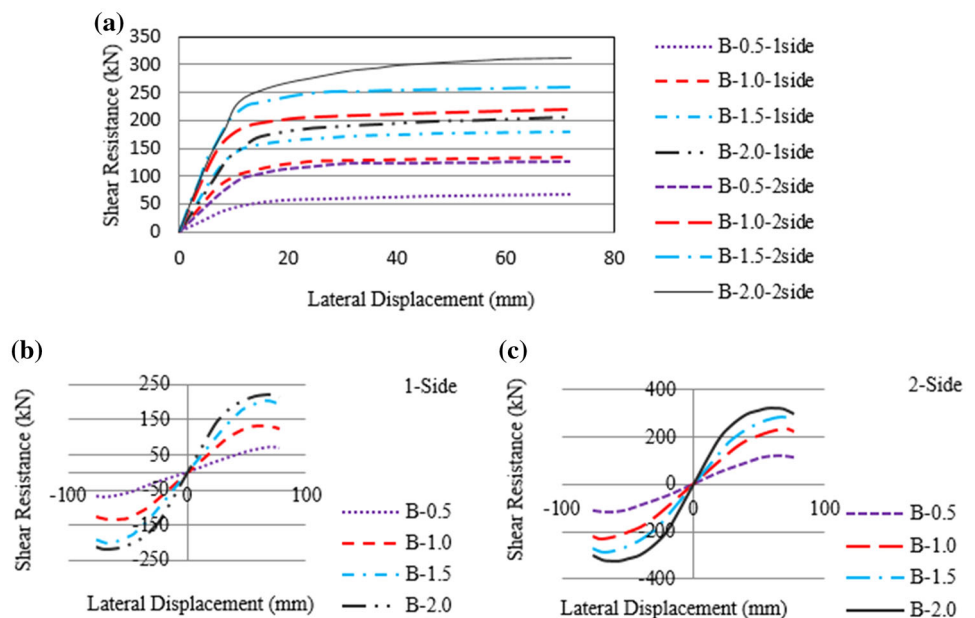
Fig. 9 Curves of specimens C.
a Monotonic curves.
b Hysteretic envelope curves,
1-side. **c** Hysteretic envelope
curves, 2-side
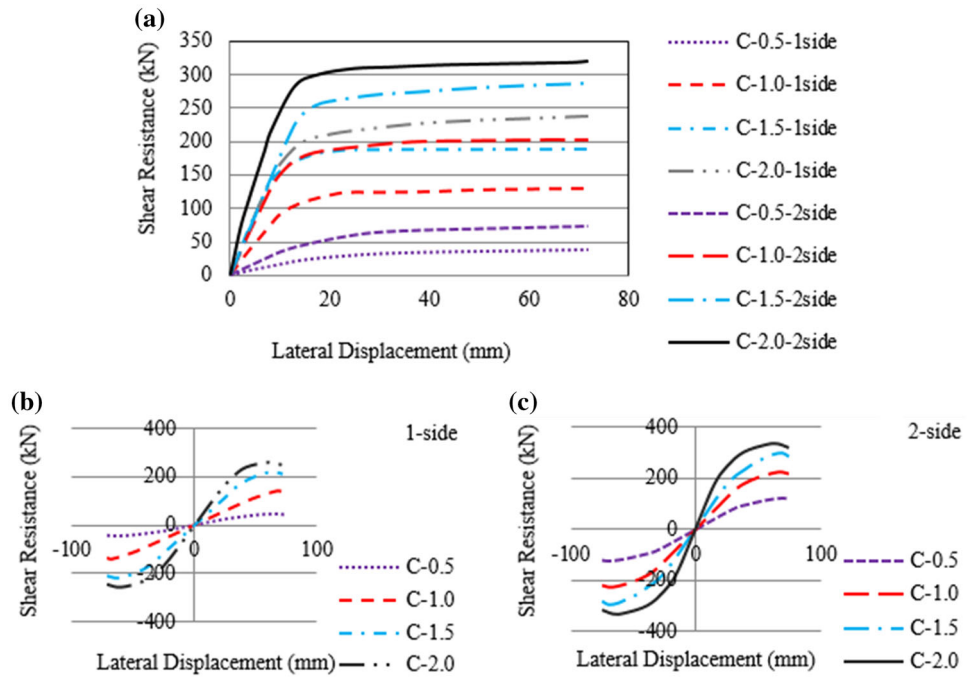
Fig. 10 Curves of specimens
D. **a** Monotonic curves.
b Hysteretic envelope curves,
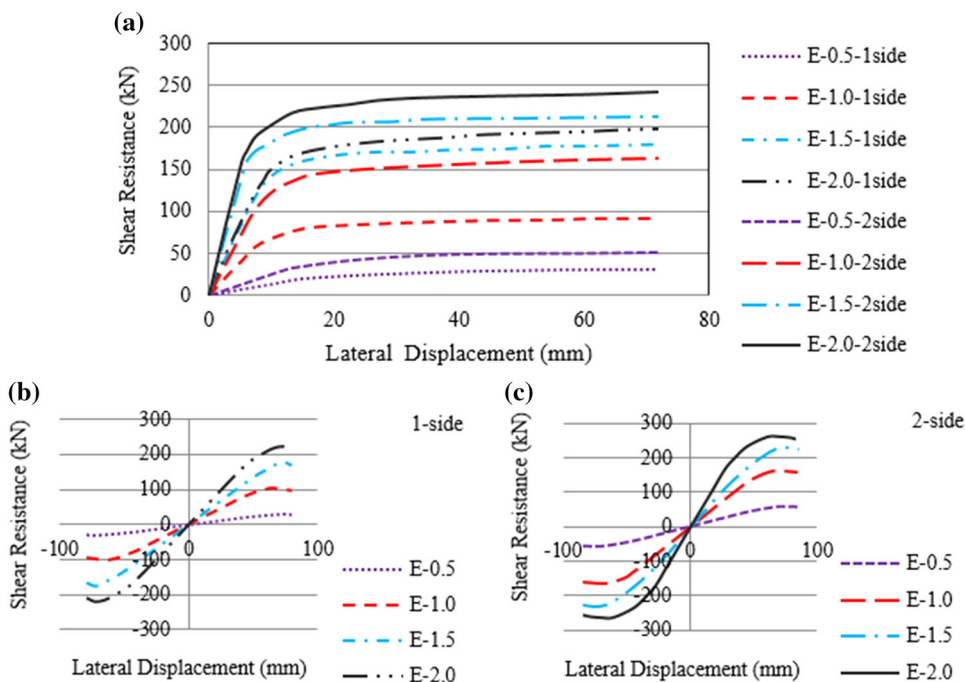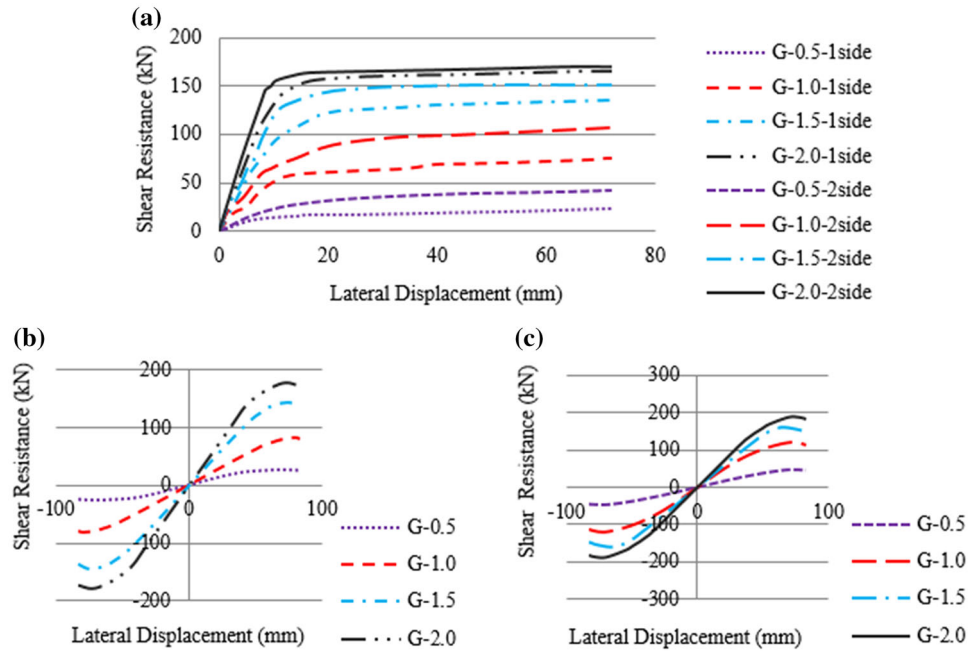1-side. **c** Hysteretic envelope
curves, 2-side
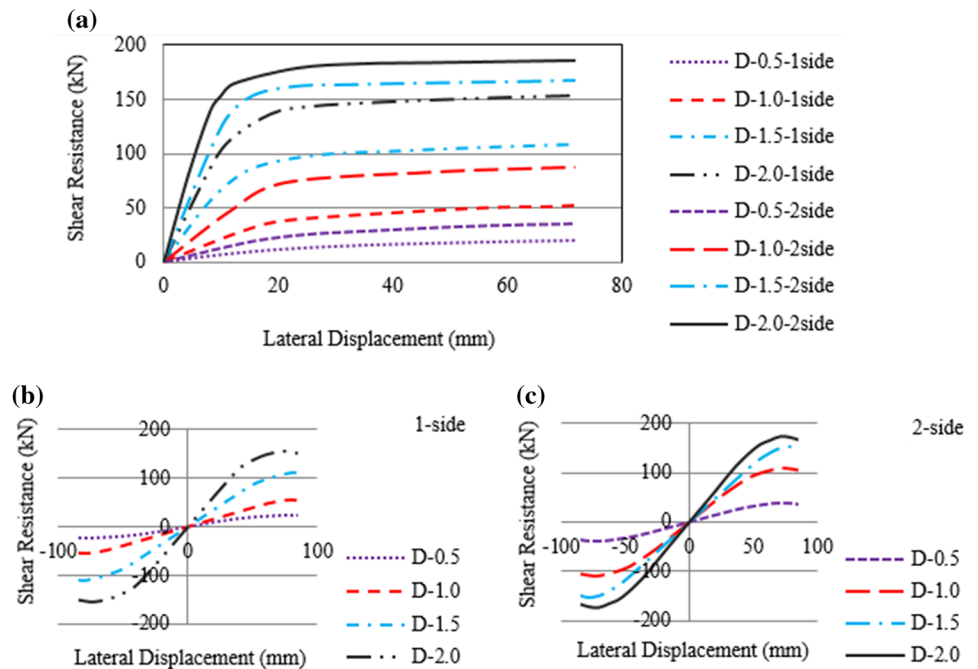
causes about 5.4 % reduction on its maximum displacement compared to lateral brace samples. The mean value of ductility was evaluated as 2.23 and 2.37, respectively (Tables 5, 6), under monotonic loading of samples F with lateral and bilateral braces and 2.36 and 2.46, respectively (Tables 7, 8), under cyclic loading. To calculate (R_d) from Eq. (3) for wall with lateral brace a mean value of ductility equal to 2.30 was used and the value of R_d was evaluated as

1.89. Since the value of (S_y/S_{yp}) is less than 1, there is no additional resistance; thus the value of (R_0) is considered equal to 1. Finally, the value of the response modification factor was obtained as 1.89 (Table 9). To calculate the value of (R_d) for wall with bilateral brace, a mean value of ductility equal to 2.42 was used and the value of R_d was evaluated as equal to 1.96. Based on values of (S_y/S_{yp}), the mean value of additional resistance (R_0) was equal to 1.45

for wall with bilateral brace and, finally, the value of the response modification factor was obtained as 2.84 for sample F with bilateral brace (Table 9). If the bilateral brace is used for sample F, the value of the response modification factor will be about 50 % more than that of the lateral brace.

The value of predicted stiffness was obtained as 17.86 and 31.95 kN/mm, respectively, for samples F with lateral and bilateral braces under monotonic loading (Tables 5, 6) and 34.53 and 36.73 kN/mm, respectively, under cyclic loading (Tables 7, 8). Obviously, the value of (K_e) is considerably less than (K_p). The shear resistance is

Fig. 11 Curves of specimens E. **a** Monotonic curves. **b** Hysteretic envelope curves, 1-side. **c** Hysteretic envelope curves, 2-side

Fig. 12 Curves of specimens F. **a** Monotonic curves. **b** Hysteretic envelope curves, 1-side. **c** Hysteretic envelope curves, 2-side
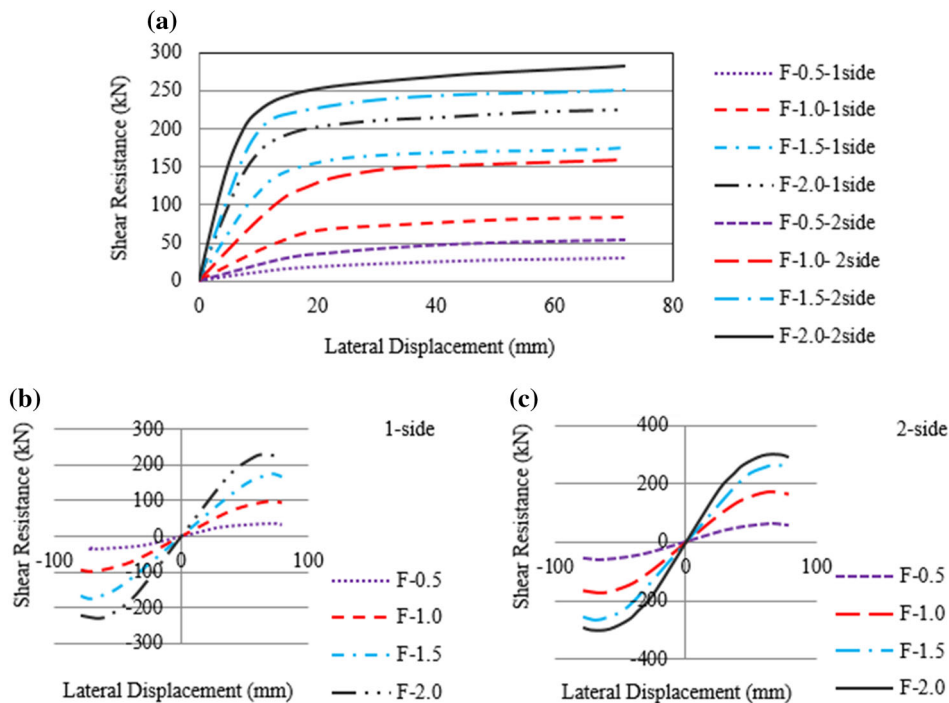
increased by increasing the ratio of the height to length of the wall. On the other hand, the shear wall resistance of bilateral brace was significantly more than that of lateral brace. This has been clearly shown in Fig. 12a–c.

Numerical analysis of frames of samples G

The mean value of yielding capacity under monotonic loading of samples G with lateral and bilateral braces was obtained as 83.23 and 95.82 kN, respectively, which has been predicted to be equivalent to 77 and 77.10 % of the capacity values (Tables 5, 6). The mean value of yielding capacity under cyclic loading of samples G with lateral and bilateral braces was obtained as 87.17 and 104.73 kN, respectively, and also the ratio of (S_y/S_{yp}) was obtained as 73.86 and 100.75 %, respectively (Tables 7, 8). The value of the yielding capacity of bilateral brace is around 18 % more than that of the lateral brace. Sample G with a lateral

Fig. 13 Curves of specimens G. a Monotonic curves. b Hysteretic envelope curves, 1-side. c Hysteretic envelope curves, 2-side

Fig. 14 Curves of specimens H. a Monotonic curves. b Hysteretic envelope curves, 1-side. c Hysteretic envelope curves, 2-side

brace could not get the total of predicted yielding capacity and, at the moment of wall failure, braces did not reach the total of the yielding capacity; however, the status of bilateral brace sample has somewhat improved compared to that of the lateral brace sample and it could get the total of predicted capacity under cyclic loading. For the ratio of yielding capacity to the nominal yielding capacity, the mean value was 79.27 and 91.26 %, respectively (Tables 5, 6), under monotonic loading of these samples with lateral and bilateral braces and 83.02 and 99.74 %, respectively (Tables 7, 8), under cyclic loading. These values show that samples G with lateral and bilateral brace could not get the expected nominal design shear resistance.

The mean value of ($\Delta_{0.8}$) was evaluated as 66.34 and 56.54 mm, respectively (Tables 5, 6), under monotonic loading of samples G with lateral and bilateral braces and 63.66 and 61.55 mm, respectively (Tables 7, 8), under cyclic loading. The presence of bilateral brace on wall causes about 9 % reduction on its maximum displacement compared to lateral brace samples. The mean value of ductility was evaluated as 2.70 and 2.75, respectively (Tables 5, 6), under monotonic loading of samples G with lateral and bilateral braces and 2.82 and 2.94, respectively (Tables 7, 8), under cyclic loading. To calculate (R_d) from Eq. (3) for wall with lateral brace, a mean value of ductility equal to 2.76 was used and the value of R_d was evaluated as 2.13. Since the value of (S_y/S_{yp}) is less than 1, there is no additional resistance; thus the value of (R_0) is considered equal to 1. Finally, the value of the response modification factor was obtained as 2.13

Fig. 15 Curves of specimens I. **a** Monotonic curves. **b** Hysteretic envelope curves, 1-side. **c** Hysteretic envelope curves, 2-side
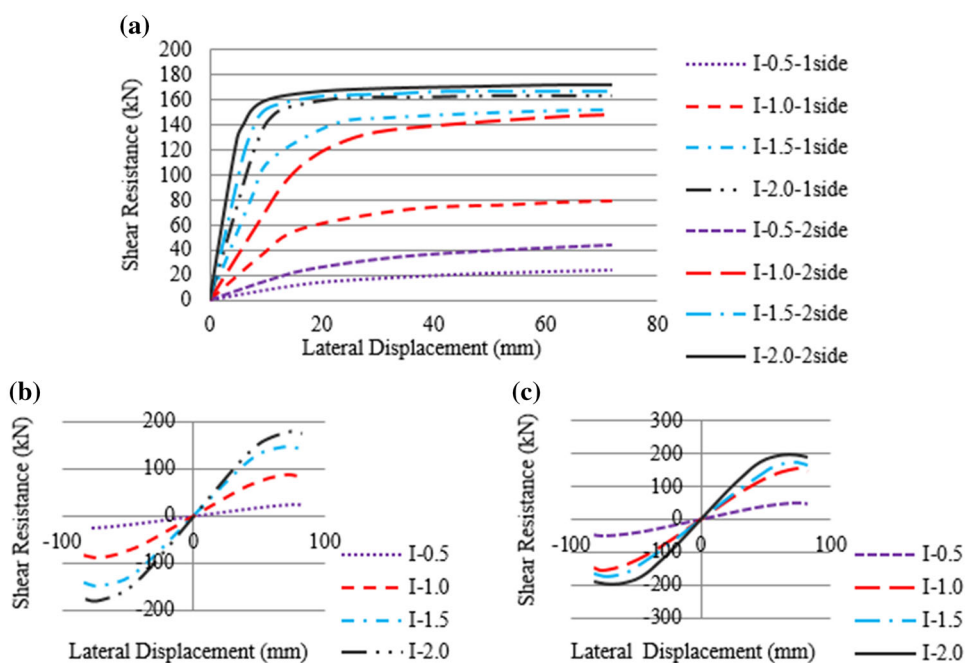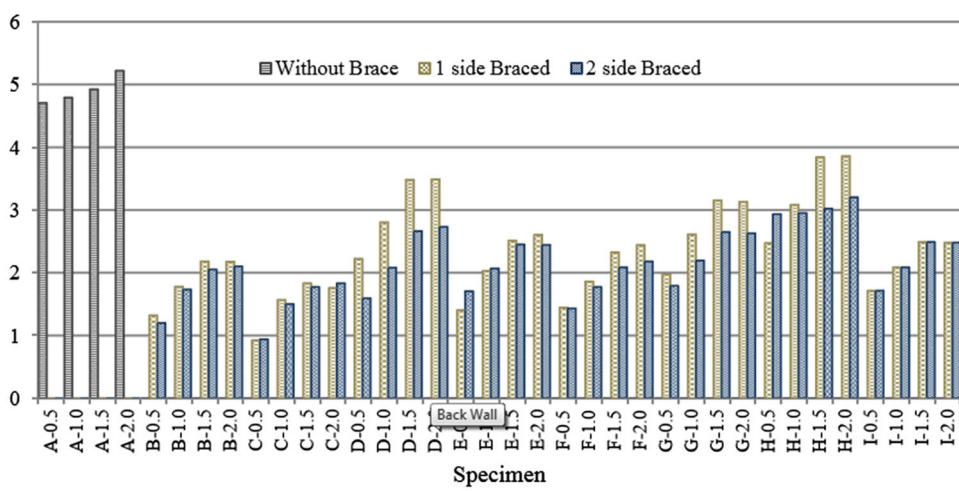

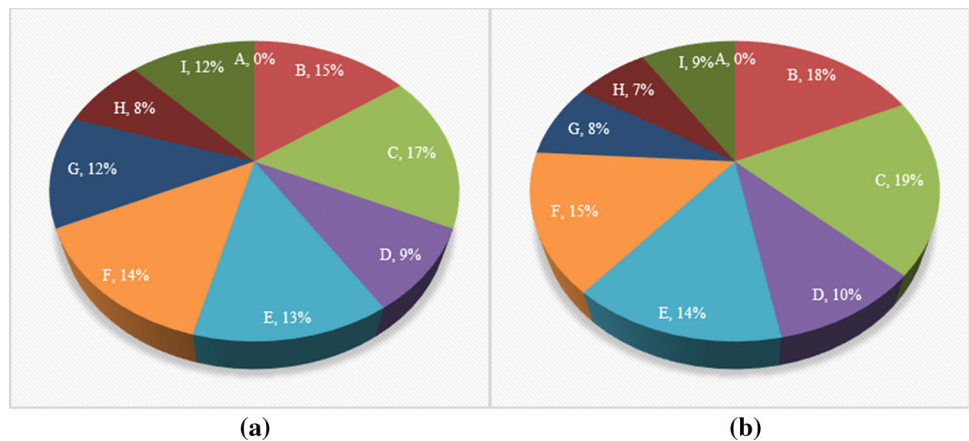Fig. 16 Comparing values of response modification factors
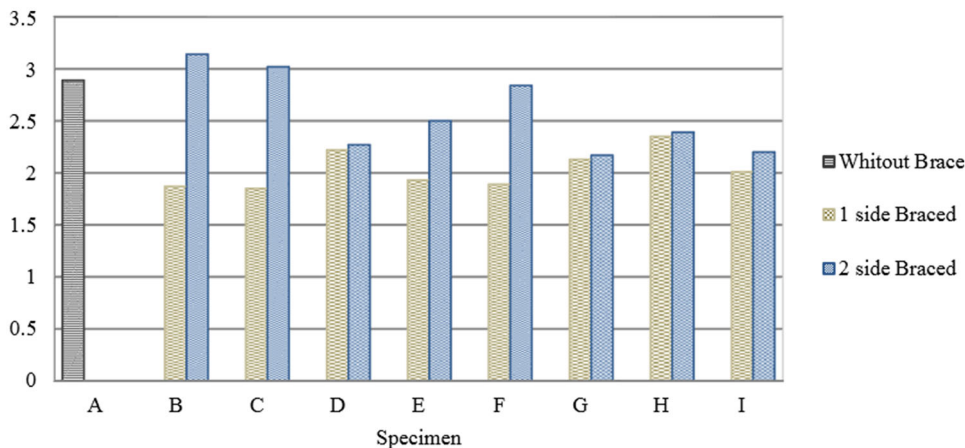
Fig. 17 Maximum strength of
the specimens (kN)
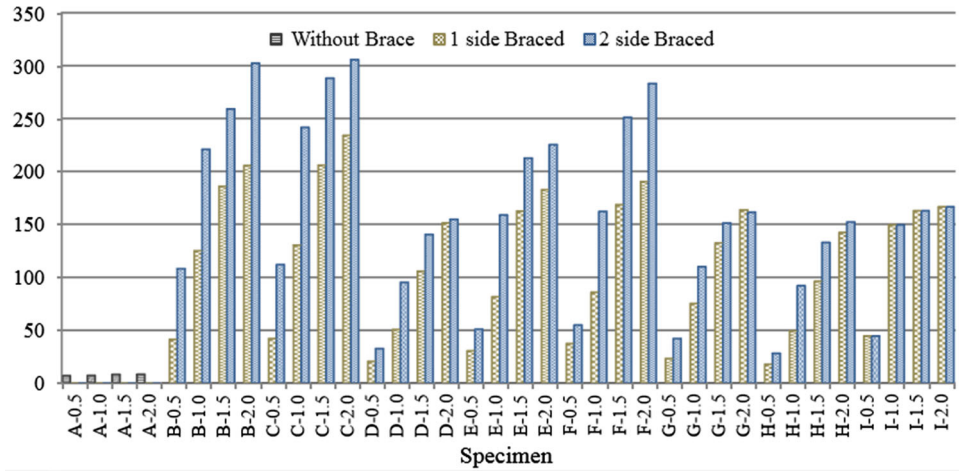
Fig. 18 Maximum lateral drift
ratio (%)

Fig. 19 Energy percent of
specimens: **a** 1-side, **b** 2-side

(a)   (b)

(Table 9). To calculate the value of (R_d) for wall with
bilateral brace, a mean value of ductility equal to 2.85
was used and the value of R_d was evaluated equal to
2.17. Since the value of (S_y/S_{yp}) is less than 1, there is no
additional resistance; thus the value of (R_0) is considered
equal to 1. Finally, the value of the response modification

factor was obtained as 2.17 for sample G with bilateral
brace (Table 9). If the bilateral brace is used for sample
G, the value of the response modification factor will be
about 1.87 % more than that of the lateral brace. This
small difference can result from the lack of additional
resistance in samples.

The value of predicted stiffness was 13.18 and 19.06 kN/mm, respectively, for samples G with lateral and bilateral braces under monotonic loading (Tables 5, 6) and 18.30 and 19.47 kN/mm, respectively, under cyclic loading (Tables 7, 8). Obviously, the value of (K_e) is considerably less than (K_p). The shear resistance is increased by increasing the ratio of the height to length of the wall. On the other hand, the shear wall resistance of the bilateral brace was significantly more than that of the lateral brace. This has been clearly shown in Fig. 13a–c.

By increasing the rate of height to length of the wall, the elastic stiffness and stiffness values are expected to increase and the amount of plasticity decreased. Using double straps will improve strength, stiffness and ductility.

Numerical analysis of frames of samples H

The mean value of yielding capacity under monotonic loading of samples H with lateral and bilateral braces was obtained as 60.49 and 83.24 kN, respectively, which has been predicted equivalent to 74.93 and 79.30 % of capacity values (Tables 5, 6). The mean value of yielding capacity under cyclic loading of samples H with lateral and bilateral braces was obtained as 64.40 and 89.38 kN, respectively, and also the ratio of (S_y/S_{yp}) was obtained as 71.90 and 114.73 %, respectively (Tables 7, 8). The value of the yielding capacity of bilateral brace is around 38 % more than that of the lateral brace. Sample H with a lateral brace could not get the total of predicted yielding capacity and, at the moment of wall failure, braces did not reach the total of the yielding capacity; however, the status of the bilateral brace sample has somewhat improved compared to that of the lateral brace sample and it could get the total of predicted capacity under cyclic loading. For the ratio of yielding capacity to the nominal yielding capacity, the mean value was 57.60 and 79.28 %, respectively (Tables 5, 6), under monotonic loading of these samples with lateral and bilateral braces and 61.33 and 85.12 %, respectively (Tables 7, 8), under cyclic loading. These values show that samples H with lateral and bilateral brace could not get the expected nominal design shear resistance.

The mean value of $(\Delta_{0.8})$ was evaluated as 80.90 and 73.89 mm, respectively (Tables 5, 6), under monotonic loading of samples H with lateral and bilateral braces and 78.90 and 76.27 mm, respectively (Tables 7, 8), under cyclic loading. The presence of bilateral brace on the wall causes about 6 % reduction on its maximum displacement compared to lateral brace samples. The mean value of ductility was evaluated as 3.16 and 3.22, respectively (Tables 5, 6), under monotonic loading of samples H with lateral and bilateral braces and 3.35 and 3.49, respectively, (Tables 7, 8) under cyclic loading. To calculate (R_d) from Eq. (3) for wall with lateral brace, a mean value of ductility

equal to 3.26 was used and the value of R_d was evaluated as 2.35. Since the value of (S_y/S_{yp}) is less than 1, there is no additional resistance; thus the value of (R_0) is considered equal to 1. Finally, the value of the response modification factor was obtained as 2.35 (Table 9). To calculate the value of (R_d) for wall with bilateral brace, a mean value of ductility equal to 3.36 was used and the value of R_d was equal to 2.39. Since the value of (S_y/S_{yp}) is less than 1, there is no additional resistance; thus the value of (R_0) is considered equal to 1. Finally, the value of the response modification factor was obtained as 2.39 for sample H with bilateral brace (Table 9). If the bilateral brace is used for sample H, the value of the response modification factor will be about 1.70 % more than that of the lateral brace. This small difference can result from the lack of additional resistance in samples.

The value of the predicted stiffness was obtained as 8.30 and 16.25 kN/mm, respectively for samples H with lateral and bilateral braces under monotonic loading (Tables 5, 6) and 11.03 and 11.74 kN/mm, respectively, under cyclic loading (Tables 7, 8). Obviously, the value of (K_e) is considerably less than (K_p). The shear resistance is increased by increasing the ratio of the height to length of the wall. On the other hand, the shear wall resistance of the bilateral brace was significantly more than the lateral brace. This has been clearly shown in Fig. 14a–c.

Numerical analysis of frames of samples I

The mean value of yielding capacity under monotonic loading of samples I with lateral and bilateral braces was 86.21 and 108.61 kN, respectively, which has been predicted equivalent to 74.73 and 78.78 % of capacity values (Tables 5, 6). The mean value of yielding capacity under cyclic loading of samples I with lateral and bilateral braces was obtained as 91.87 and 116.92 kN, respectively, and also the ratio of (S_y/S_{yp}) was obtained as 74.67 and 112.10 %, respectively (Tables 7, 8). The value of the yielding capacity of bilateral brace was around 26 % more than that of the lateral brace. sample I with a lateral brace could not get the total of predicted yielding capacity and, at the moment of wall failure, braces did not reach the total of the yielding capacity; however, the status of bilateral brace sample has somewhat improved compared to that of lateral brace sample and it could get the total of predicted capacity under cyclic loading. For the ratio of yielding capacity to the nominal yielding capacity, the mean value was 82.11 and 103.44 %, respectively (Tables 5, 6), under monotonic loading of these samples with lateral and bilateral braces and 87.49 and 11.35 %, respectively (Tables 7, 8), under cyclic loading. These values show that samples I with bilateral brace could get the expected nominal design shear resistance well.

The mean value of ($\Delta_{0.8}$) was evaluated as 57.75 and 53.53 mm, respectively (Tables 5, 6), under monotonic loading of samples I with lateral and bilateral braces and 56.42 and 54.55 mm, respectively (Tables 7, 8) mm under cyclic loading. The presence of bilateral brace on wall causes about 5.3 % reduction on its maximum displacement compared to lateral brace samples. The mean value of ductility was evaluated as 2.23 and 2.37, respectively (Tables 5, 6), under monotonic loading of samples I with lateral and bilateral braces and 2.36 and 2.46, respectively (Tables 7, 8), under cyclic loading. To calculate (R_d) from Eq. (3) for wall with lateral brace, a mean value of ductility equal to 2.52 was used and the value of R_d was evaluated as 2.01. Since the value of (S_y/S_{yp}) is less than 1, there is no additional resistance; thus the value of (R_0) is considered equal to 1. Finally, the value of the response modification factor was obtained as 2.01 (Table 9). To calculate the value of (R_d) for wall with bilateral brace, a mean value of ductility equal to 2.62 was used and the value of R_d was equal to 2.06. Based on values of (S_y/S_{yp}), the mean value of additional resistance (R_0) was equal to 1.07 for the wall with bilateral brace and, finally, the value of the response modification factor was 2.20 for sample I with bilateral brace (Table 9). If the bilateral brace is used for sample I, the value of the response modification factor will be about 9.45 % more than that of the lateral brace. This small difference can result from the lack of additional resistance in samples.

The value of predicted stiffness was 14.58 and 19.57 kN/mm, respectively, for samples I with lateral and bilateral braces under monotonic loading (Tables 5, 6) and 20.79 and 22.11 kN/mm, respectively, under cyclic loading (Tables 7, 8). Obviously, the value of (K_e) is considerably less than (K_p). The shear resistance is increased by increasing the ratio of the height to length of the wall. On the other hand, the shear wall resistance of bilateral brace was significantly more than the lateral brace. This has been clearly shown in Fig. 15a–c.

By increasing the rate of height to length of wall, the elastic stiffness and stiffness values are expected to increase and the amount of plasticity decreased. Using double straps will improve strength, stiffness and ductility.

Comparing values of response modification factors for samples

The results relating to values of the response modification factor for all samples have been collected in Table 9 and its diagram can be qualitatively observed in Fig. 16. Sample B with bilateral brace was allocated the highest value of response modification factor.

Comparing maximum drift and resistance of the samples

A qualitative comparison has been given in Figs. 17 and 18 to compare the maximum resistance and drift of samples at a glance. As it is clear, samples with bilateral brace include maximum value of resistance and samples without brace have minimum value of resistance. Among samples with bilateral brace, sample C with dimension ratio of 2 has the highest value of resistance. However, samples without brace have the maximum value of drift and samples with bilateral brace have the lowest drift.

Comparing the mean energy contribution of the samples

The energy absorption capability in sample C is on average more than that of the other samples, and this shows that for sample C, reduction in the resistance stiffness and erosion is lower than that of the other samples. From Fig. 19a–b, it may be noted that the value of energy absorbed in the sample without brace is insignificant compared to other samples.

Conclusions

Among the studied samples, sample C was allocated the maximum mean of yielding resistance, S_y, the highest mean of predicted stiffness and the highest percentage of energy absorption capability. It is clear that the minimum value of these parameters was related to sample A that was wall without brace. The maximum and minimum mean ratio of S_y/S_{yp} was related to samples A and D, respectively. The maximum and minimum mean ratio of S_y/S_{yp} was also observed in samples C and A, respectively. In wall without brace, the maximum and minimum drifts were observed in samples A and C, respectively. Generally, samples with lateral brace could not get total of predicted yielding capacity and, at the moment of wall failure, braces did not reach the total yielding capacity; however, the status of bilateral brace samples has somewhat improved compared to that of lateral brace samples and could get the total predicted capacity in cyclic tests. In both modes of unilateral and bilateral braces, samples C and B have been able to gain the predicted nominal design shear resistance. Also, in the mode of bilateral brace, sample F could get the expected nominal design shear resistance well, and in the mode of lateral brace, it largely succeeded, but not entirely. Samples E and I could obtain the expected nominal design shear resistance only in bilateral brace mode. In all samples, the value of K_e was considerably less than that of K_p.

In bilateral brace, the maximum response modification factor was 3.14 for sample B and 2.35 for sample H. It was also observed that the presence of lateral or bilateral brace had no significant difference in the value of response modification factor for samples D, G, H and I. In the wall without brace, a high ductility was observed compared to the other samples, but no additional resistance was observed in this sample. In all samples, the shear resistance increased by increasing the ratio of wall height to length and the shear resistance of wall with bilateral brace was 60 % more than the lateral brace.

References

AISI (2001a) Standard for cold-formed steel framing—prescriptive method for one and two family dwelling. American Iron and Steel Institute, Washington, DC

AISI (2001b) North American specification for the design of cold-formed steel structural members. American Iron and Steel Institute, Washington, DC

Al-Kharat M, Rogers CA (2007) Inelastic performance of cold-formed steel strap braced walls. J Constr Steel Res 63(4):460–474

AS/NZS4600 (2005) Cold-formed steel structures. Australian Building Codes Board, Canberra

ASCE7-05 (2005) ASCE7-05 minimum design loads for buildings and other structures, American Society of Civil Engineers

ASTM E2126 (2005) Standard test methods for cyclic (reversed) load test for shear resistance of framed walls for buildings. ASTM International, West Conshohocken

ASTM-E2126-07 (2007) Standard test methods for cyclic (reversed) load test for shear resistance of walls for buildings. USA, p 13

Berman JW, Celik OC, Bruneau M (2005) Comparing hysteretic behavior of light-gauge steel plate shear walls and braced frames. Eng Struct 27(3):475–485

Dabreo J, Balh N, Ong-Tone C, Rogers CA (2014) Steel sheathed cold-formed steel framed shear walls subjected to lateral and gravity loading". Thin Walled Struct 74:232–245

FEMA-450 (2003) NEHRP recommended provisions for seismic regulations for new buildings and other structures—part 1 provisions. Building Seismic Safety Council, USA

FEMA-P750 (2009) NEHRP recommended seismic provisions for new buildings and other structures. Building Seismic Safety Council, Washington, DC

Fiorino L, Iuorio O, Landolfo R (2012) Seismic analysis of sheathing-braced cold-formed steel structures. Eng Struct 34:538–547

Fülöp LA, Dubina D (2004) Performance of wall-stud cold-formed shear panels under monotonic and cyclic loading part I: experimental research. Thin Walled Struct 42(2):321–338

Gad EF, Chandler AM, Duffield CF, Hutchinson GL (1999a) Earthquake ductility and overstrength in residential structures. J Struct Eng Mech 8(4):361–382

Gad EF, Duffield CF, Hutchinson GL, Mansell DS, Stark G (1999b) Lateral performance of cold-formed steel-framed domestic structures. J Eng Struct 21(1):83–95

Kim TW, Wilcoski J, Foutch DA, Lee MS (2006) Shaketable tests of a cold-formed steel shear panel. J Eng Struct 28(10):1462–1470

Miller TH, Pekoz T (1993) Behavior of cold-formed steel wall stud assemblies. J Struct Eng 119(3):641–651

Moghimi H, Ronagh HR (2009) Performance of light-gauge cold-formed steel strap-braced stud walls subjected to cyclic loading. Eng Struct 31(1):69–83

MSC Software (2012) MSC Nastran 2012 Users Guide. MSC Software

National Research Council of Canada (NRCC) (2005) National Building Code of Canada. Ottawa, ON

Newmark N, Hall W (1982) Earthquake spectra and design. Earthquake Engineering Research Institute, Berkeley, California, p 170

Nithyadharan M, Kalyanaraman V (2012) Modelling hysteretic behaviour of cold-formed steel wall panels. Eng Struct 46:643–652

Pan ChL, Shan MY (2011) Monotonic shear tests of cold-formed steel wall frames with sheathing. Thin Walled Struct 49:363–370

Serrette RL (1997) Additional shear wall values for light weight steel framing Report No. LGSRG-1-97, Santa Clara University, Santa Clara, CA

Telue T, Mahendran M (2002) Behavior of cold-formed steel wall frames lined with plasterboard. J Constr Steel Res 57(4):435–452

TI 809–07 (1998) Design of cold-formed loadbearing steel systems and masonry veneer/steel stud walls. US Army Corps of Engineers, Engineering and Construction Division, USA

Zeynalian M, Ronagh HR (2010a) Performance of K-braced cold-formed steel shear walls subjected to lateral cyclic loading. In: Zingoni A (ed) Advances and trends in structural engineering mechanics and computation. CRC Press, London

Zeynalian M, Ronagh HR (2010b) Performance of knee braced cold-formed steel shear walls subjected to lateral cyclic loading. In: Proceedings of the 20th international specialty conference for cold-formed steel structures, Missouri University of Science and Technology, St. Louis, MO

Zeynalian M, Ronagh HR (2011) A numerical study on seismic characteristics of knee-braced cold formed steel shear walls. Thin Walled Struct 49:1517–1525

Zeynalian M, Ronagh HR (2012a) A numerical study on seismic performance of strap-braced cold-formed steel shear walls. Thin-Walled Struct 60:229–238

Zeynalian M, Ronagh HR (2012b) A numerical study on seismic characteristics of knee-braced cold formed steel shear walls. Thin Walled Struct 49:1517–1525

Zeynalian M, Ronagh HR, Hatami S (2012) Seismic characteristics of K-braced cold-formed steel shear walls. J Constr Steel Res 77:23–31